RESEARCH MEMORANDUM

A STUDY OF THE APPLICATION OF AIRFOIL SECTION DATA TO THE ESTIMATION OF THE HIGH-SUBSONIC-SPEED CHARACTERISTICS OF SWEPT WINGS

By Lynn W. Hunton

Ames Aeronautical Laboratory
Moffett Field, Calif.

[redacted]

NATIONAL ADVISORY COMMITTEE
FOR AERONAUTICS

WASHINGTON

June 24, 1955

[redacted]

NATIONAL ADVISORY COMMITTEE FOR AERONAUTICS

RESEARCH MEMORANDUM

A STUDY OF THE APPLICATION OF AIRFOIL SECTION DATA TO THE ESTIMATION OF THE HIGH-SUBSONIC-SPEED CHARACTERISTICS OF SWEPT WINGS

By Lynn W. Hunton

SUMMARY

Estimates of the variation with Mach number of the aerodynamic characteristics of swept wings are made on the basis of airfoil section data combined with span-loading theory. The analysis deals with examinations of some 26 wings and wing-body combinations ranging in sweep angle from 30° to 60° and for Mach numbers between 0.6 and 1.0.

Results of the study indicate that the two-dimensional section data afford good qualitative information for such high-speed aerodynamic characteristics as the variation with Mach number of drag, zero-lift pitching-moment coefficient, and lift coefficient for flow separation. Quantitative estimates of the force and moment divergence Mach numbers could not be made with any degree of certainty from the airfoil data alone. Somewhat improved quantitative estimates for a given configuration were obtainable by basing the estimates on the measured characteristics for a wing of similar plan form but different section, and adjusting for the effects of differences in section on the basis of section data.

INTRODUCTION

At low values of lift where the viscous problems of flow separation are minimized, wing span-loading theory, such as that developed in references 1 and 2, has been found to handle rather successfully the span-loading changes associated with sweep throughout the subcritical Mach number range. Estimates, therefore, of the lift and moment characteristics of swept wings in the linear range should pose little difficulty to the aircraft designer. However, a quantitative definition of the actual limits of this low-lift linear range are not to be found from the theory itself. Nor at higher values of lift and Mach number where problems of viscosity and supercritical flow are encountered will

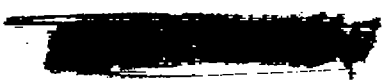

potential theory provide the information required by the aircraft designer. Consequently, studies of existing flight and wind-tunnel data are held essential for purposes of gaining not only a further understanding of the aerodynamic problems involved with swept wings but also to develop, if possible, improved methods for estimating the characteristics of an arbitrary swept-wing design.

For flows essentially incompressible, the work of references 3 and 4 demonstrated the value of combining two-dimensional data with span-loading theory for estimating the loading and stalling behavior of two 45° sweptback wings. In view of the measure of success found at the lower speeds, this general program has been extended to the compressible-flow case, crude as the assumptions obviously are for handling such a complex flow problem, in an attempt to determine to just what extent high-speed two-dimensional airfoil data could be linked to the characteristics of the finite wing. The findings of one such study dealing with the detail loadings on a 45° sweptback wing of aspect ratio 6 have been reported in reference 5. In the present report the analysis is centered around the three-component force and moment data for some 26 different wing and wing-body combinations covering angles of sweepback from 30° to 60° and Mach numbers from about 0.6 to 1.0. The test Reynolds numbers of the three-dimensional data included in the survey fall generally within a range of 2 to 4 million.

NOTATION

C_L	lift coefficient, $\frac{\text{lift}}{qS}$
C_{L_α}	lift-curve slope at zero lift, $\frac{dC_L}{d\alpha}$
C_D	drag coefficient, $\frac{\text{drag}}{qS}$
C_{D_i}	induced drag based on reference 1
C_m	pitching-moment coefficient, $\frac{\text{pitching moment}}{qS\bar{c}}$
C_{m_o}	pitching-moment coefficient at zero lift
M	free-stream Mach number
M_Λ	free-stream Mach number for yawed wing, equal to M
M_D	Mach number for drag divergence, M at which $\frac{dC_D}{dM} = 0.1$

P	pressure coefficient
R	Reynolds number based on $\bar{c}$
S	wing area
a	mean-line designation
b	wing span
c	local chord measured parallel to plane of symmetry
$\bar{c}$	wing mean aerodynamic chord, $\frac{\int_0^{b/2} c^2 dy}{\int_0^{b/2} c\, dy}$
c_d	section drag coefficient, $\frac{\text{section drag}}{qc}$
c_l	section lift coefficient, $\frac{\text{section lift}}{qc}$
c_{l_α}	section lift-curve slope, $\frac{dc_l}{d\alpha}$
c_{l_i}	design section lift coefficient
c_{m_o}	section pitching moment at zero lift
q	free-stream dynamic pressure
x	chordwise distance from leading edge measured parallel to plane of symmetry
y	spanwise distance measured normal to plane of symmetry
α	angle of attack
ϵ	angle of twist (positive for washin)
η	fraction of semispan
Λ	sweep angle of wing quarter-chord line

Wing notation, see table I

Subscripts

calc	calculated
exp	experimental
max	maximum
sep	trailing-edge flow separation
Λ	yawed flow

METHODS AND APPLICATION

In estimating the characteristics of a finite-span wing, two different procedures will be considered. For the first, all three-dimensional effects are assumed to be confined to span loading; hence, in such a scheme local sections are considered to behave like infinite-span sections. This general approach was employed in reference 6 for unswept wings and subsequently served as the groundwork for a study of a swept wing in incompressible flow reported in reference 3. In the present analysis directed at the subsonic compressible-flow case, this method has been simplified still further by ignoring the variations in local loading across the span in evaluating the compressibility and viscosity effects. In other words, the evaluations of these effects are based on the airfoil section data for a lift coefficient corresponding to the average wing lift coefficient. The yawed infinite-wing data were derived from unswept two-dimensional airfoil data using simple-sweep-theory relations with no allowances for any root, tip, or body interference effects. Procedural details followed in estimating the variations with Mach number of C_{L_α}, C_D, C_{m_o}, and C_L for beginning of flow separation are indicated in subsequent paragraphs. This method will be referred to as the adjusted wing theory procedure.

In the second procedure considered herein, incremental differences found from the two-dimensional data are applied to the known characteristics for a three-dimensional configuration approximating the one in question but differing primarily in airfoil section. This method, which will be referred to as the adjusted wing data procedure, obviously has the advantage of including in the estimate the three-dimensional interference effects omitted in the first procedure.

A summary of the wing configurations considered, together with the references from which the data were extracted (refs. 7 to 30), is given in table I.

Adjusted Wing Theory Procedure

Lift-curve slope.- Wing lift-curve-slope variation with Mach number was calculated from span-loading theory using the method of reference 1. In the supercritical Mach number range where the theory fails to indicate sufficient increase, the theoretical values have been adjusted percentage-wise by the amount that the two-dimensional lift-curve-slope data exceed the rise given by the Prandtl-Glauert factor $\frac{1}{\sqrt{1 - M^2}}$. The Mach numbers for the two-dimensional data were related to those for the wing through the sweep-theory relation

$$M_{\Lambda=0} = M_{\Lambda} \cos \Lambda$$

A correlation of these results is given in figure 1 for 26 swept-wing configurations. In each case, the estimates are based on data for airfoil section configurations approximating the assumed effective section of the swept wing taken normal to the wing quarter-chord line.

Drag.- The estimated values of total drag were determined using the expression

$$C_D = c_{d_o} \cos \Lambda + \Delta c_d \cos^3 \Lambda + C_{D_i}$$

where

c_{d_o} section minimum drag coefficient (assumed to be skin-friction drag and effect of sweep estimated from ref. 31)

Δc_d section pressure-drag coefficient, $c_d - c_{d_o}$, at $c_{l_{\Lambda=0}} = \frac{C_L}{\cos^2 \Lambda}$ and $M_{\Lambda=0} = M_{\Lambda} \cos \Lambda$

c_d section drag coefficient at c_l and M indicated above

C_{D_i} induced drag coefficient calculated using reference 1

For all the wing-alone configurations, the estimated drag values were determined from the above expression directly. For the wing-fuselage combinations, a fixed incremental drag of 0.0050 was added to the estimates to facilitate comparison of Mach number effects. These results are summarized in figure 1.

Zero-lift pitching moment.- As indicated previously, estimates at zero lift of wing pitching-moment coefficient due to camber are based directly on the equivalent two-dimensional value adjusted for sweep

effects. Thus, the moment for the cambered swept wing without twist is assumed equal to that for the cambered section in yawed flow

$$C_{m_o} = c_{m_{o_\Lambda}} = c_{m_{o_{\Lambda=o}}} \cos^2\Lambda$$

for Mach numbers adjusted as before so that

$$M_\Lambda = \frac{M_{\Lambda=o}}{\cos \Lambda}$$

For wings having twist in addition to camber, the final total C_{m_o} consists of the sum of that associated with the basic loading due to twist (calculated from ref. 1) and that due to camber indicated above. These results are shown in figure 1.

Lift coefficient for flow separation.- A study of the pressure distributions of various airfoil sections at high Mach number revealed that the incidence of flow separation (that is, failure of pressures on the upper surface to recover fully at the trailing edge) is closely allied with the section $c_{l_{max}}$ for Mach numbers up to a certain critical value. This is illustrated in figure 2 for a 14.3-percent-thick symmetrical NACA 64-series airfoil which was found to be typical of all airfoils studied with the exception of those with large amounts of camber, that is, a design lift coefficient of 0.4 or higher. At the critical Mach number mentioned the flow separation changes from one associated with the normal breakdown of flow near $c_{l_{max}}$ to one induced by the adverse pressure gradients due to the normal shock. Hence, in the present analysis the two indicated lines, one for $c_{l_{max}}$ and the other for shock-induced stall illustrated in figure 2, have been assumed to define the lift versus Mach number boundaries for flow separation for a given airfoil. Assuming the three-dimensional wing to evidence flow separation at a C_L equivalent to that for the yawed infinite airfoil, then

$$C_{L_{sep}} = c_{l_{sep_\Lambda}} = c_{l_{sep_{\Lambda=o}}} \cos^2\Lambda$$

for Mach numbers of the wing governed by

$$M_\Lambda = \frac{M_{\Lambda=o}}{\cos \Lambda}$$

Since variations in the slope of the pitching-moment curve usually provide a rather sensitive indication of the start of breakdown of the flow on the swept wing, this quantity has been used herein in an attempt to evaluate the accuracy of the flow-separation estimates. Correlations of the estimated values of C_L for flow separation with the pitching-moment data are given in figure 3 for the various wings considered.

For those few wings for which pressure-distribution data were available there is also included on the pitching-moment curve a point indicating the measured C_L for beginning of trailing-edge flow separation as determined from the pressure data.

Adjusted Wing Data Procedure

For this procedure, as stated previously, the estimates of the characteristics for a given configuration start with the known three-dimensional data for a configuration approximating as closely as possible that in question. The first step is to adjust these known results to account for any differences in plan-form and twist effects using some span-loading method such as reference 1. Whatever differences exist in airfoil section between the two configurations then are accounted for by applying to the known characteristics increments that have been determined from the high-speed data for the two airfoil sections, following the sweep-theory relations outlined in the foregoing paragraphs.

DISCUSSION

Adjusted Wing Theory Procedure

The fundamental concept of two-dimensional flow prevailing at local sections of the finite wing overlooks the changes in loading at the root and tip associated with plan form and the additional changes in pressure distribution in these regions due to compressibility effects. These changes in loading are briefly illustrated in figure 4 for a 35° swept-back wing. Shown in the figure are comparisons of the pressure distributions measured at several Mach numbers and span stations of the wing with those estimated for the yawed infinite airfoil based on pressure measurements obtained on the airfoil in the Ames 1- by 3-1/2-foot high-speed tunnel. In each example the estimated pressure diagram has been determined for the equivalent value of local lift coefficient and Mach number in unswept flow and the resultant values of pressure coefficient then converted to yawed-flow conditions such that

$$P_\Lambda = P_{\Lambda=0}\cos^2\Lambda$$

thus, the measured and estimated pressure-diagram areas are equal. It may be seen in the figure that although quite large differences in the measured and estimated loadings occurred at the root and tip, the two-dimensional data offer rather accurate loading information over the wing mid-semispan for Mach numbers well into the supercritical flow region. A more detailed study of the limits of applicability of two-dimensional data to estimating the local loading characteristics for a 45° swept wing is given in reference 5.

In studying the surface-loading characteristics of a number of swept wings it became evident that the shifts in loading at the root and tip had generally an equal and opposite effect insofar as the over-all force characteristics of the finite swept wing were concerned. Furthermore, extensive flow separation on the swept wing was found to be delayed until the average of the values of local c_l (rather than the peak c_l as for unswept wings) reached the two-dimensional value for flow separation. Consequently, the aerodynamic characteristics of the swept wing tend to exhibit the characteristics of the average section of the wing. It would be expected, therefore, that yawed-infinite-airfoil data should be generally representative of the behavior of the swept finite wing.

Lift-curve slope.- The results of figure 1 showing the measured variation of C_{L_α} with Mach number as compared to those calculated by the method of reference 1 indicate reasonably accurate estimates up to about the critical Mach number. Above this Mach number the calculated values fail to indicate sufficient rate of increase. The deficiency can to some extent be traced to the inability of the Prandtl-Glauert small-perturbation theory (employed in the span loading method of reference 1) to account in full for the lift-curve-slope changes measured at supercritical speeds in two-dimensional flow. By adjusting the calculated slope as follows,

$$C_{L_\alpha} = \frac{(C_{L_\alpha})_{calc} \, (c_{l_\alpha})_{exp} \sqrt{1 - M^2}}{\left[(c_{l_\alpha})_{exp}\right]_{M=0}}$$

some improvement can be made in the estimated lift-curve slopes[1] for wings of 35° sweep (see fig. 1). Here the sweep-angle value is not so great but what the flow reaches supercritical conditions normal to the isobars prior to the entrance of the wing into the three-dimensional sonic-flow regime beginning at a Mach number of about 0.95. Such is not the case, however, for wings of 40° sweep or higher where a sufficient amount of sweep exists to delay critical conditions on the section to Mach numbers beyond the 0.95 limit where the three-dimensional sonic-flow system commences to engulf the entire wing-fuselage configuration. Obviously for sweep angles beyond about 40° then, the two-dimensional data can be of little benefit for purposes of improving the calculated lift-curve slopes at low values of lift.

[1]In computing the wing lift-curve slopes by reference 1, the two-dimensional c_{l_α} data could have been substituted in place of the theoretical slope $2\pi/\sqrt{1 - M^2}$ used therein. However, this practice is not recommended since the majority of measured incompressible lift-curve slopes fall somewhat below the theoretical slope of 2π. For some unaccountable reason, much more accurate results are obtainable using the base theoretical slope of 2π and correcting that by the measured deficiency in the supercritical region.

Drag.- Comparisons of estimated and measured variations of drag coefficient with Mach number for fixed values of wing lift coefficient are given in figure 1. It is seen from these results that the variations of drag with Mach number were indicated with reasonable accuracy up to Mach numbers approaching those for drag divergence even for lift coefficients where considerable flow separation must have been present (e.g., wing 7, fig. 1(c)). The estimated drag-divergence Mach numbers, on the other hand, as well as magnitude of drag level must be considered insufficiently accurate for most design purposes. A summary of the estimated and measured drag-divergence Mach numbers is given in figure 5. For wings of about 35° sweep the estimated values show a deviation of as much as 10 percent while with further increase in sweep angle the correlation points depart rather abruptly from the line of perfect correlation to follow a new path which approaches a measured M_D limit line of about 0.95. Hence, it is clear that as long as the drag divergence of the wing is governed by section characteristics (such as for wings with 35° sweep or less) a rather rough estimate of M_D is possible with this method, but that an upper limit exists for M_D in the neighborhood of 0.95 caused by three-dimensional sonic-flow conditions (onset of wave drag). This boundary cannot be altered by further increase in sweep or changes in section other than by their contribution to a change in the longitudinal distribution of area. The effects of such changes in area on drag at sonic speeds are discussed in reference 32.

Zero-lift pitching moment.- Included in figure 1 are the estimates of C_{m_o} for those wings having camber either alone or combined with twist. Where two-dimensional data were not available for the exact section normal to the quarter-chord line of the wing, the closest section available has been substituted and the estimate adjusted proportionately where necessary in order to match exactly the absolute magnitudes of camber. It can be seen that while the magnitude and variation of C_{m_o} with Mach number could be estimated reasonably well, again for most of the swept wings the divergence Mach number fell near or beyond the Mach number 0.95 limit, thus rendering the method unreliable for such purposes in this speed range.

Flow separation.- Flow separation as used herein refers primarily to the trailing-edge type (unless stated otherwise) where the pressures fail to recover fully at the trailing edge. Flow separation on the swept wing marks the beginning of large increases in drag and local changes in lift which usually result in unacceptable variations in pitching moment, the severity of this latter effect being dependent on the wing plan form. For swept wings these changes accompanying flow separation occur at lift coefficients somewhat below $C_{L_{max}}$ with buffeting and the variations in pitching moment usually being of such magnitude as to effectively limit the useful lift range of the wing at this point. At transonic speeds the separation can stem from adverse pressure gradients arising not only from the effects of thickness and circulation as at low speed, but from the effects of compressibility and shocks as well. For the former type,

fairly reliable estimates of flow separation on swept wings can be made using two-dimensional airfoil data as demonstrated at low speed in references 3 and 33, and at high speed in reference 5. For estimating separation induced by shock waves, it would be anticipated that equally good results could be achieved with the two-dimensional data provided the shock on the finite wing was associated with velocity perturbations in planes normal to the isobars and not from the three-dimensional shock system that engulfs the configuration as a whole near sonic speed. A detailed study of the extent to which two-dimensional loads data can be correlated with the local loading on a 45° sweptback wing has been made in reference 5. In the present report the problem has been viewed somewhat differently; for a large number of wings estimates have been made of the C_L for flow separation based on two-dimensional data in an attempt to show what relation, if any, this estimated $C_{L_{sep}}$ has with the observed wing C_L for pitch divergence.

The pitching-moment characteristics together with the estimated values of $C_{L_{sep}}$ for the wings considered in the study are shown in figure 3. For the few wings for which pressure-distribution data were available for determining when flow separation actually began, a measured value for $C_{L_{sep}}$ has also been indicated on the pitching-moment curve. These measured values of $C_{L_{sep}}$ serve to show (aside from the obvious comparison with the estimated $C_{L_{sep}}$ values) that the pitching-moment variations are at best only a rough guide to flow separation. One of the better illustrations of this point is found in wing 5 (fig. 3(a)) where changes in pitching moment are seen to occur initially at a lift coefficient of about 0.2 (described in ref. 10 as due to a boundary-layer transition phenomenon) whereas actually the pressure-distribution data showed no evidence of flow separation until a C_L of about 0.5 (Mach number of 0.6) where a second change in slope of the pitching-moment curve occurred. It is this measured value of $C_{L_{sep}}$ that can be seen to agree very closely with the estimated value for $C_{L_{sep}}$ determined from airfoil section data. In general, the other values of estimated $C_{L_{sep}}$ also show quite satisfactory agreement with the measured values. A review of all of the estimates of $C_{L_{sep}}$ in relation to the pitching-moment characteristics will show that some change in slope of the pitching-moment curve usually occurred near the estimated C_L for flow separation. On the basis of these comparisons as well as those involving the measured values of $C_{L_{sep}}$, it is apparent that the airfoil section data do afford a fairly reliable indication of the lift coefficient for onset of extensive flow separation. Unfortunately, however, this indicated success does not guarantee that a change in moment will not also occur at some lower lift coefficient. Nor is there any reliable method available at the present time to predict with certainty which direction an anticipated change in moment will pitch the airplane - up, down, or not at all. Nevertheless, it is believed the correlation as shown in figure 3 covering a large

number of wings is of particular value in providing some insight into the interpretation of the observed pitching-moment disturbances of swept wings.

Adjusted Wing Data Procedure

In developing improved designs the process usually entails consideration of changes to a given basic configuration for which some amount of experimental aerodynamic data exist. Since a considerable amount of three-dimensional data are now available in the literature, plan-form effects can for the most part be estimated from existing data. Any effects of airfoil section differences then can be readily accounted for by using the same sweep-theory relations outlined in the previous paragraphs. To illustrate this point, figure 6 has been prepared showing a comparison of the estimated and measured variation of drag coefficient with Mach number for several of the configurations for which it was possible to isolate changes in section for a given plan form (see table I for description of configurations). For example, the estimated drag characteristics given for wing 3 in figure 6(a) were derived from the measured drag data for wing 2 as a base to which were added the incremental differences in drag found from the two-dimensional drag measurements (appropriately adjusted for sweep effects) for the two airfoil sections of these wings. The estimated results for wings 8, 17, 13, 16, and 15 also included in figure 6 have been based on the measured data for wings 5, 23, 14, 14, and 22, respectively. In comparing these correlations with those of figure 1 it may be seen that somewhat improved estimates of drag-divergence Mach number can be made using this procedure.

Some additional drag characteristics are presented in figure 7 in the form of profile-drag-coefficient variation with lift coefficient. Using these data it is possible to compare the incremental differences between the profile-drag curves for the two different wings based on the yawed-infinite-airfoil data (labeled "Estimated") and on the finite-wing data (labeled "Measured"). Shown in the figure for several Mach numbers are the effects of section modification for four example wings and one example of the effect of a plan-form sweep-angle change of 30° to 45°, wings 9 and 18. In all cases the agreement between the two- and three-dimensional results is quite good.

In figure 8 are presented plots of incremental changes in lift coefficient for flow separation as a function of Mach number for the wings dealt with in figure 7. For the comparisons the estimated and measured increments have been derived from the results of figure 3. For three of the wings presented (5, 15, and 22) the measured increments were based on the known values of $C_{L_{sep}}$ found from pressure-distribution data whereas for the remainder of the wings recourse was made to the pitch divergence characteristics as a rough guide to the start of flow

separation. It is interesting to note from these results, as well as the profile-drag curves of figure 7, the contrast in effectiveness of the leading-edge modification (wings 2 and 3) as compared to a uniform-type camber (e.g., wings 22 and 15) as a function of both Mach number and lift coefficient. The superior effectiveness of the uniform-type camber from a lift and drag standpoint are quite accurately predicted from the airfoil section data.

CONCLUDING REMARKS

With the use of high-speed airfoil section data, estimates have been made of some of the aerodynamic characteristics of 26 swept wings with consideration being given to two different procedures. In one the finite-wing characteristics were related to airfoil section data while in the second method, the estimates were based on the known data for a finite wing approximating the configuration in question with increments then applied to account for the differences in airfoil section. While the first method did not provide too reliable an indication of absolute magnitudes, particularly the drag level and force- and moment-divergence Mach numbers, the method did afford surprisingly good qualitative indications of the variations with Mach number of drag, zero-lift pitching moment, and lift coefficient for flow separation for Mach numbers up to about 0.9. Application of the second method showed considerable improvement in the estimated values of drag-divergence Mach number and lift coefficient for flow separation.

Ames Aeronautical Laboratory
National Advisory Committee for Aeronautics
Moffett Field, Calif., Mar. 23, 1955

REFERENCES

1. DeYoung, John, and Harper, Charles W.: Theoretical Symmetric Span Loading at Subsonic Speeds for Wings Having Arbitrary Plan Form. NACA Rep. 921, 1948.

2. DeYoung, John: Theoretical Symmetric Span Loading Due to Flap Deflection for Wings of Arbitrary Plan Form at Subsonic Speeds. NACA Rep. 1071, 1952.

3. Hunton, Lynn W.: Effects of Finite Span on the Section Characteristics of Two 45° Sweptback Wings of Aspect Ratio 6. NACA TN 3008, 1953.

4. Hunton, Lynn W., and James, Harry A.: Use of Two-Dimensional Data in Estimating Loads on a 45° Sweptback Wing With Slats and Partial-Span Flaps. NACA TN 3040, 1953.

5. Walker, Harold J., and Maillard, William C.: A Correlation of Airfoil Section Data With the Aerodynamic Loads Measured on a 45° Sweptback Wing Model at Subsonic Mach Numbers. NACA RM A55C08, 1955.

6. Anderson, Raymond F.: Determination of the Characteristics of Tapered Wings. NACA Rep. 572, 1936.

7. Henry, Beverly Z.: A Transonic Wing Investigation in the Langley 8-Foot High-Speed Tunnel at High Subsonic Mach Numbers and at a Mach Number of 1.2 - Wing-Fuselage Configuration Having a Wing of 35° Sweepback, Aspect Ratio 4, Taper Ratio 0.6, and NACA 65A006 Airfoil Section. NACA RM L50J09, 1950.

8. Demele, Fred A., and Sutton, Fred B.: The Effects of Increasing the Leading-Edge Radius and Adding Forward Camber on the Aerodynamic Characteristics of a Wing With 35° of Sweepback. NACA RM A50K28a, 1951.

9. Kelly, John A., and Hayter, Nora-Lee F.: Aerodynamic Characteristics of a Leading-Edge Slat on a 35° Swept-Back Wing for Mach Numbers From 0.30 to 0.88. NACA RM A51H23, 1951.

10. Tinling, Bruce E., and Lopez, Armando E.: The Effects of Reynolds Number at Mach Numbers up to 0.94 on the Loading on a 35° Swept-Back Wing Having NACA 651A012 Streamwise Sections. NACA RM A52B20, 1952.

11. Tinling, Bruce E., and Kolk, W. Richard: The Effects of Mach Number and Reynolds Number on the Aerodynamic Characteristics of Several 12-Percent-Thick Wings Having 35° of Sweepback and Various Amounts of Camber. NACA RM A50K27, 1951.

12. Bielat, Ralph P.: A Transonic Wind-Tunnel Investigation of the Aerodynamic Characteristics of Three 4-Percent-Thick Wings of Sweepback Angles 10.8°, 35°, and 47°, Aspect Ratio 3.5, and Taper Ratio 0.2 in Combination with a Body. NACA RM L52B08, 1952.

13. Whitcomb, Richard T.: An Investigation of the Effects of Sweep on the Characteristics of a High-Aspect-Ratio Wing in the Langley 8-Foot High-Speed Tunnel. NACA RM L6J01a, 1947.

14. Bray, Richard S.: The Effects of Fences on the High-Speed Longitudinal Stability of a Swept-Wing Airplane. NACA RM A53F23, 1953.

15. Boddy, Lee E.: Investigation at High Subsonic Speeds of Methods of Alleviating the Adverse Interference at the Root of a Swept-Back Wing. NACA RM A50E26, 1950.

16. Goodson, Kenneth W., and Few, Albert G., Jr.: Effect of Leading-Edge Chord-Extensions on Subsonic and Transonic Aerodynamic Characteristics of Three Models Having 45° Sweptback Wings of Aspect Ratio 4. NACA RM L52K21, 1953.

17. Bielat, Ralph P., Harrison, Daniel E., and Coppolino, Domenic A.: An Investigation at Transonic Speeds of the Effects of Thickness Ratio and of Thickened Root Sections on the Aerodynamic Characteristics of Wings with 47° Sweepback, Aspect Ratio 3.5, and Taper Ratio 0.2 in the Slotted Test Section of the Langley 8-foot High-Speed Tunnel. NACA RM L51I04a, 1951.

18. Boltz, Frederick W., and Kolbe, Carl D.: The Forces and Pressure Distribution at Subsonic Speeds on a Cambered and Twisted Wing Having 45° of Sweepback, an Aspect Ratio of 3, and a Taper Ratio of 0.5. NACA RM A52D22, 1952.

19. Johnson, Ben H., Jr., and Shibata, Harry H.: Characteristics Throughout the Subsonic Speed Range of a Plane Wing and of a Cambered and Twisted Wing, Both Having 45° of Sweepback. NACA RM A51D27, 1951.

20. Edwards, George G., Tinling, Bruce E., and Ackerman, Arthur C.: The Longitudinal Characteristics at Mach Numbers up to 0.92 of a Cambered and Twisted Wing Having 40° of Sweepback and an Aspect Ratio of 10. NACA RM A52F18, 1952.

21. Osborne, Robert S., and Mugler, John P., Jr.: Aerodynamic Characteristics of a 45° Sweptback Wing-Fuselage Combination and the Fuselage Alone Obtained in the Langley 8-Foot Transonic Tunnel. NACA RM L52E14, 1952.

22. Runckel, Jack F., and Schmeer, James W.: The Aerodynamic Characteristics at Transonic Speeds of a Model With a 45° Sweptback Wing, Including the Effect of Leading-Edge Slats and a Low Horizontal Tail. NACA RM L53J08, 1954.

23. Kolbe, Carl D., and Boltz, Frederick W.: The Forces and Pressure Distribution at Subsonic Speeds on a Plane Wing Having 45° of Sweepback, an Aspect Ratio of 3, and a Taper Ratio of 0.5. NACA RM A51G31, 1951.

24. Reynolds, Robert M., and Smith, Donald W.: Aerodynamic Study of a Wing-Fuselage Combination Employing a Wing Swept Back 63° - Subsonic Mach and Reynolds Number Effects on the Characteristics of the Wing and on the Effectiveness of an Elevon. NACA RM A8D20, 1948.

25. Wiggins, James W., and Kuhn, Richard E.: Wind-Tunnel Investigation of the Aerodynamic Characteristics in Pitch of Wing-Fuselage Combinations at High-Subsonic Speeds - Sweep Series. NACA RM L52D18, 1952.

26. Hemenover, Albert D.: Tests of the NACA 64-010 and 64A010 Airfoil Sections at High Subsonic Mach Numbers. NACA RM A9E31, 1949.

27. Van Dyke, Milton Denman: High-Speed Subsonic Characteristics of 16 NACA 6-Series Airfoil Sections. NACA TN 2670, 1952.

28. Stivers, Louis S., Jr.: Effects of Subsonic Mach Number on the Forces and Pressure Distributions on Four NACA 64A-Series Airfoil Sections at Angles of Attack as High as 28°. NACA TN 3162, 1954.

29. Summers, James L., and Treon, Stuart L.: The Effects of Amount and Type of Camber on the Variation With Mach Number of the Aerodynamic Characteristics of a 10-Percent-Thick NACA 64A-Series Airfoil Section. NACA TN 2096, 1950.

30. Hemenover, Albert D.: The Effects of Camber on the Variation With Mach Number of the Aerodynamic Characteristics of a 10-Percent-Thick Modified NACA Four-Digit-Series Airfoil Section. NACA TN 2998, 1953.

31. Young, A. D., and Booth, T. B.: The Profile Drag of Yawed Wings of Infinite Span. Aero. Quart., Nov. 1951, pp. 211-229.

32. Whitcomb, Richard T.: A Study of Zero-Lift Drag Chacteristics of Wing-Body Combinations Near the Speed of Sound. NACA RM L52H08, 1952.

33. Maki, Ralph L.: The Use of Two-Dimensional Section Data To Estimate the Low-Speed Wing Lift Coefficient at Which Section Stall First Appears on a Swept Wing. NACA RM A51E15, 1951.

TABLE I.- WING CONFIGURATIONS AND DATA SOURCES

Wing	Configuration[a]	NACA section		Reference	
		Definition	Used	Wing	Section
1	35-4-.6-WF	65A006 ∥	65-008	7	unpub.
2	35-4.5-.5-W	64A010 ⊥	64A010	8	26
3	35-4.5-.5-W	64A010 ⊥ (mod. L.E.)[b]	64A010 (mod.L.E.)	8	unpub.
4	35-4.8-.51-WF	0011.56-64 (mod.) ⊥	0011.56-64 (mod.)	9	unpub.
5	35-5.1-.71-W	65A012 ∥	64A0(14.3)	10	unpub.
6	35-10-.5-W	65A012 ∥	64A0(14.3)	11	unpub.
7	35-3.5-.2-WF	65A004 ∥ (1/3 230; 0.1 c_{l_i} a=1)	65-206	12	27
8	35-5.1-.71-W	64A312 ∥	65-412	11	unpub.
9	30-7.4-.38-WF	65-210 ⊥	65-210	13	27
10	35-4.8-.51-WFT	0011.56-64 (mod.) ⊥	0011.56-64 (mod.)	14	unpub.
11	36-6-.5-WF	64A015 ⊥	64A0(14.3)	15	unpub.
12	45-4-.3-WF	65A006 ∥	65-008	16	unpub.
13	47-3.5-.2-WF	65A004 ∥ (1/3 230; 0.1 c_{l_i} a=1)	65-206	17	27
14	47-3.5-.2-WF	65A006 ∥ (1/3 230; 0.1 c_{l_i} a=1)	65-208	17	27
15	45-3-.5-W (ϵ = -5°)	64A410 ⊥	64A410	18	28
16	47-3.5-.2-WF	65A009 ∥ (1/3 230; 0.1 c_{l_i} a=1)	65-212	17	27
17	45-5-.57-W (ϵ = -8.7°)	64A810 ⊥	64A910	19	29
18	45-5.1-.38-WF	65-210 ⊥	65-210	13	27
19	40-10-.4-W (ϵ = -5°)	0014-0011 ⊥ (c_{l_i}=0.4 a=0.8)	0010-1.10 40/1.051 (c_{l_i}=0.4 a=0.8)	20	30
20	45-4-.6-WF	65A006 ∥	65-008	21	unpub.
21	45-3.56-.3-WF	64A007 ∥	64A010	22	26
22	45-3-.5-W	64A010 ⊥	64A010	23	26
23	45-5-.57-W	64A010 ⊥	64A010	19	26
24	45-5.5-.5-WF	64A010 ⊥	64A010	5	26
25	63-3.5-.25-W	64A006 ∥	64A010	24	26
26	60-4-.6-WF	65A006 ∥	64A010	25	26

[a]Configuration given in following order: sweepback angle, aspect ratio, taper ratio, and wing, wing-fuselage, or wing-fuselage-tail combination.

[b]Modified leading edge.

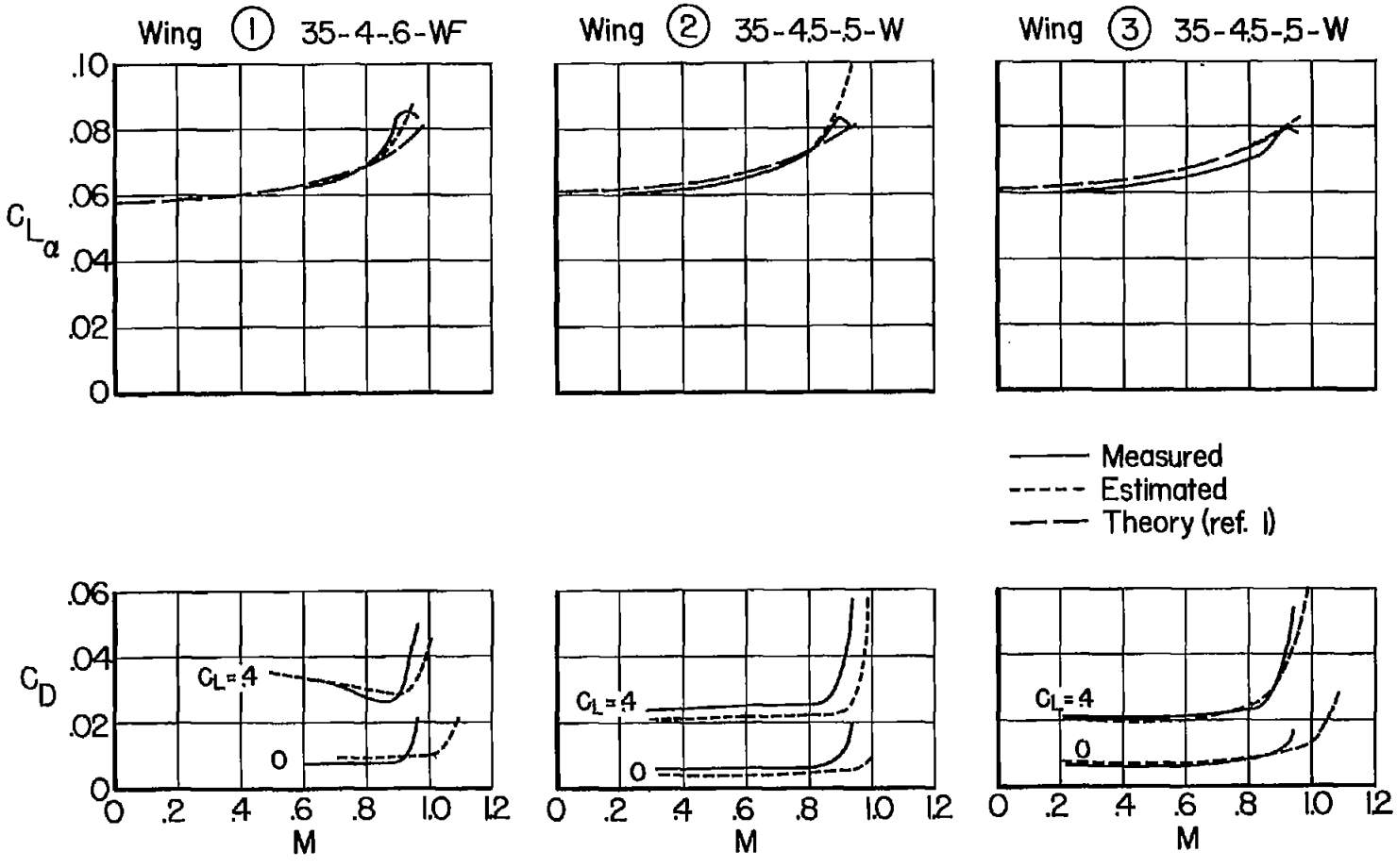

(a) Wings 1 to 3

Figure 1.- Comparisons of the measured and estimated characteristics of the swept wings determined by the adjusted wing theory procedure.

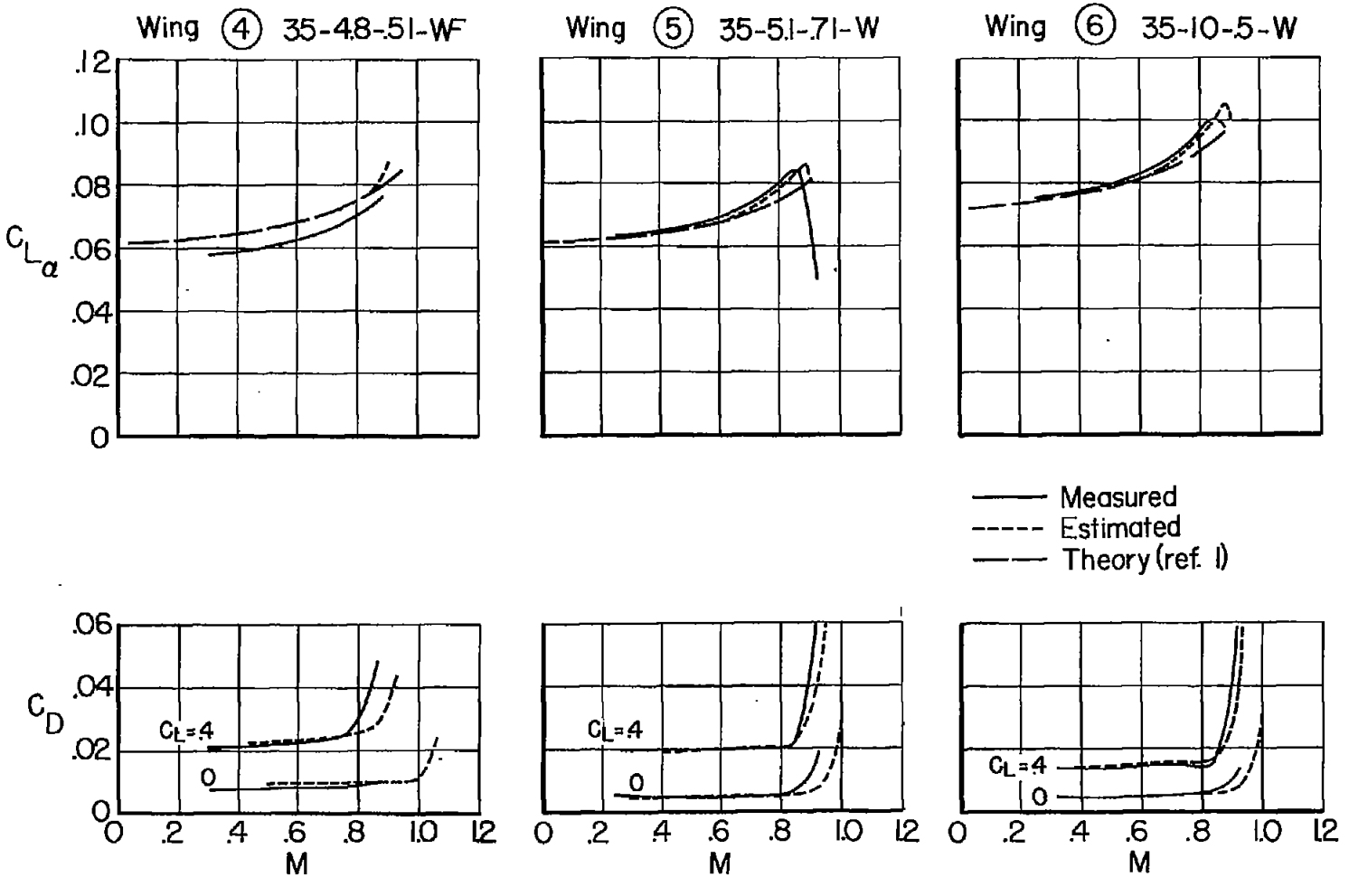

(b) Wings 4 to 6

Figure 1.- Continued.

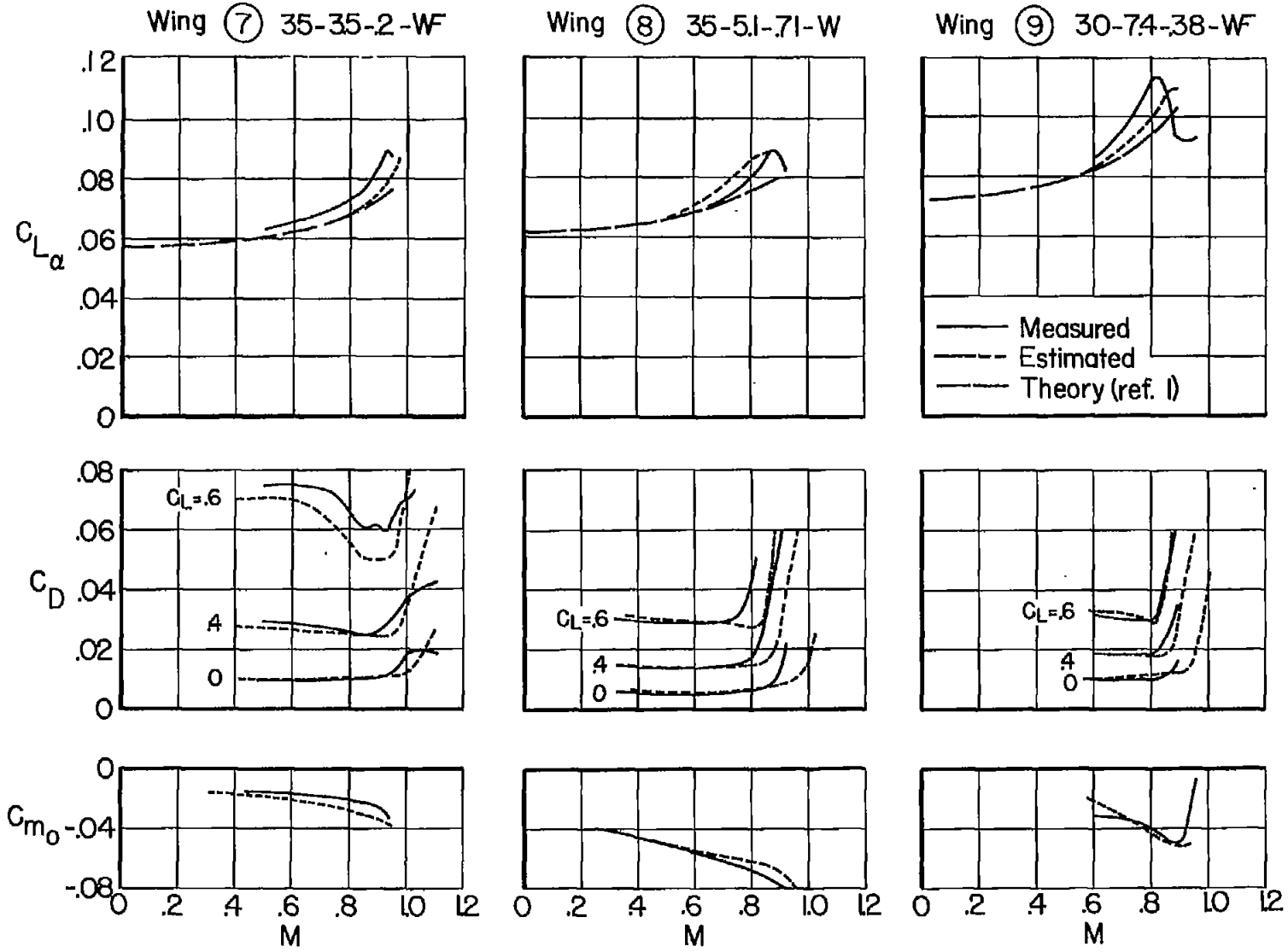

(c) Wings 7 to 9

Figure 1.- Continued.

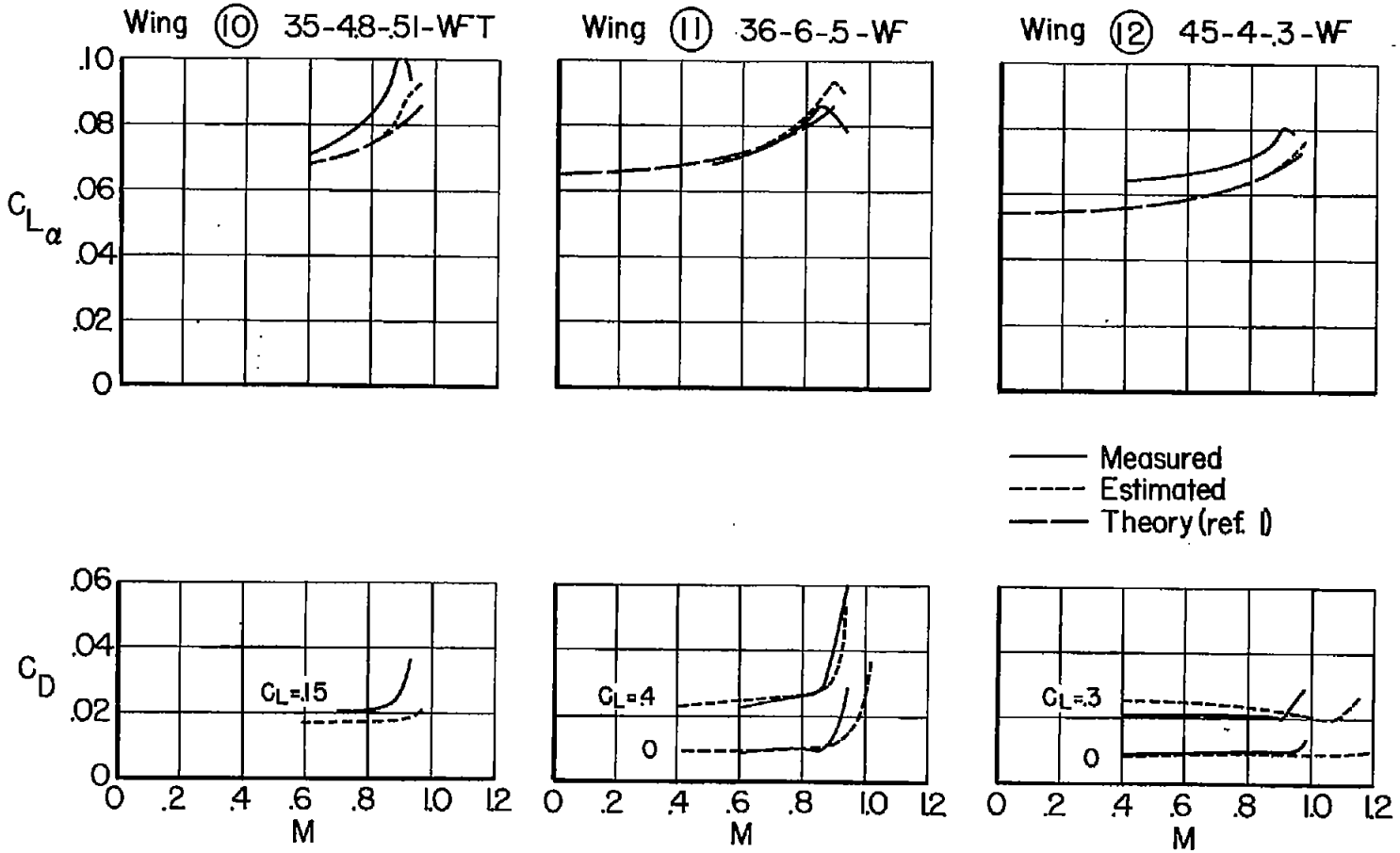

(d) Wings 10 to 12

Figure 1.- Continued.

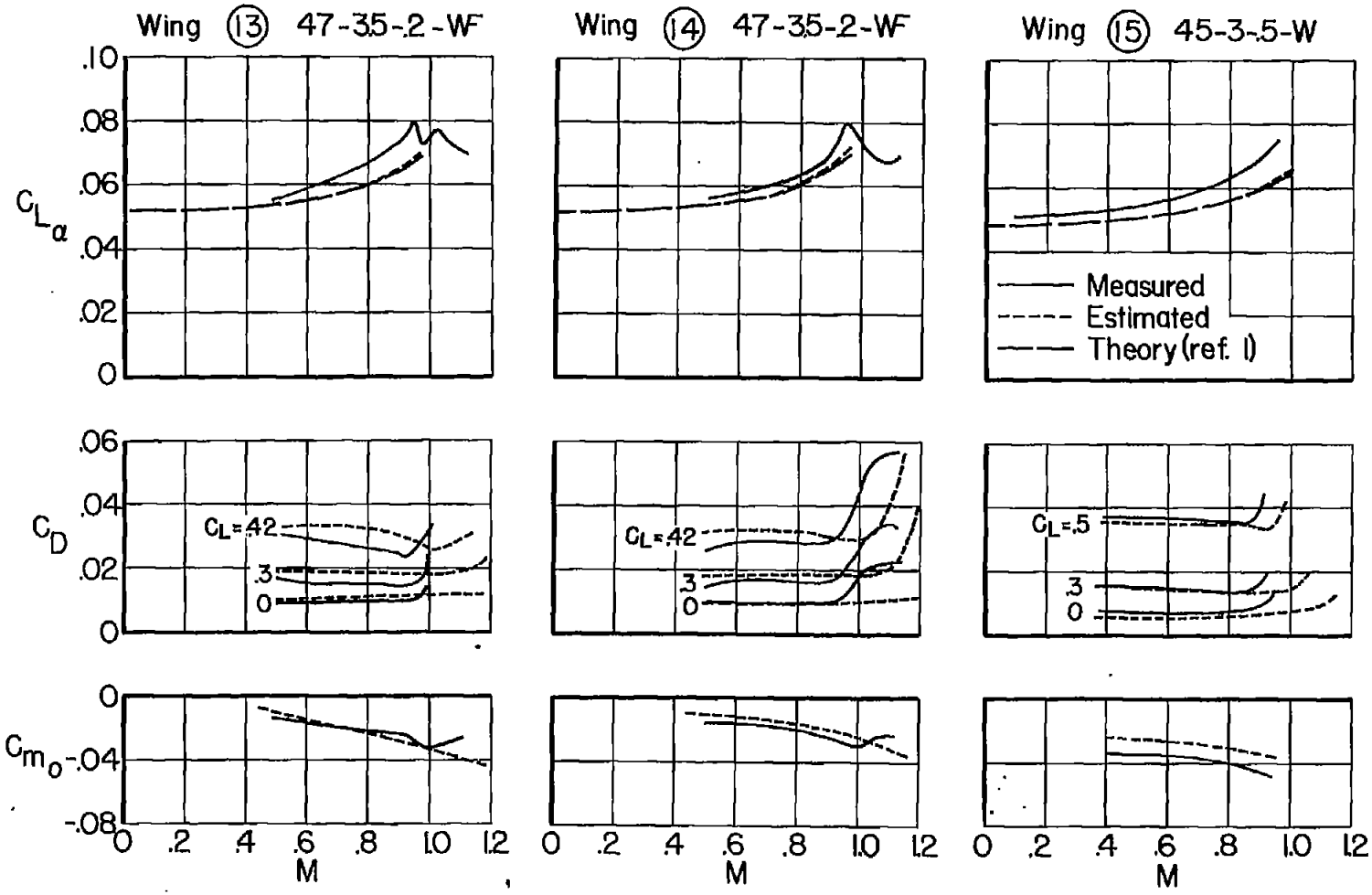

(e) Wings 13 to 15

Figure 1.- Continued.

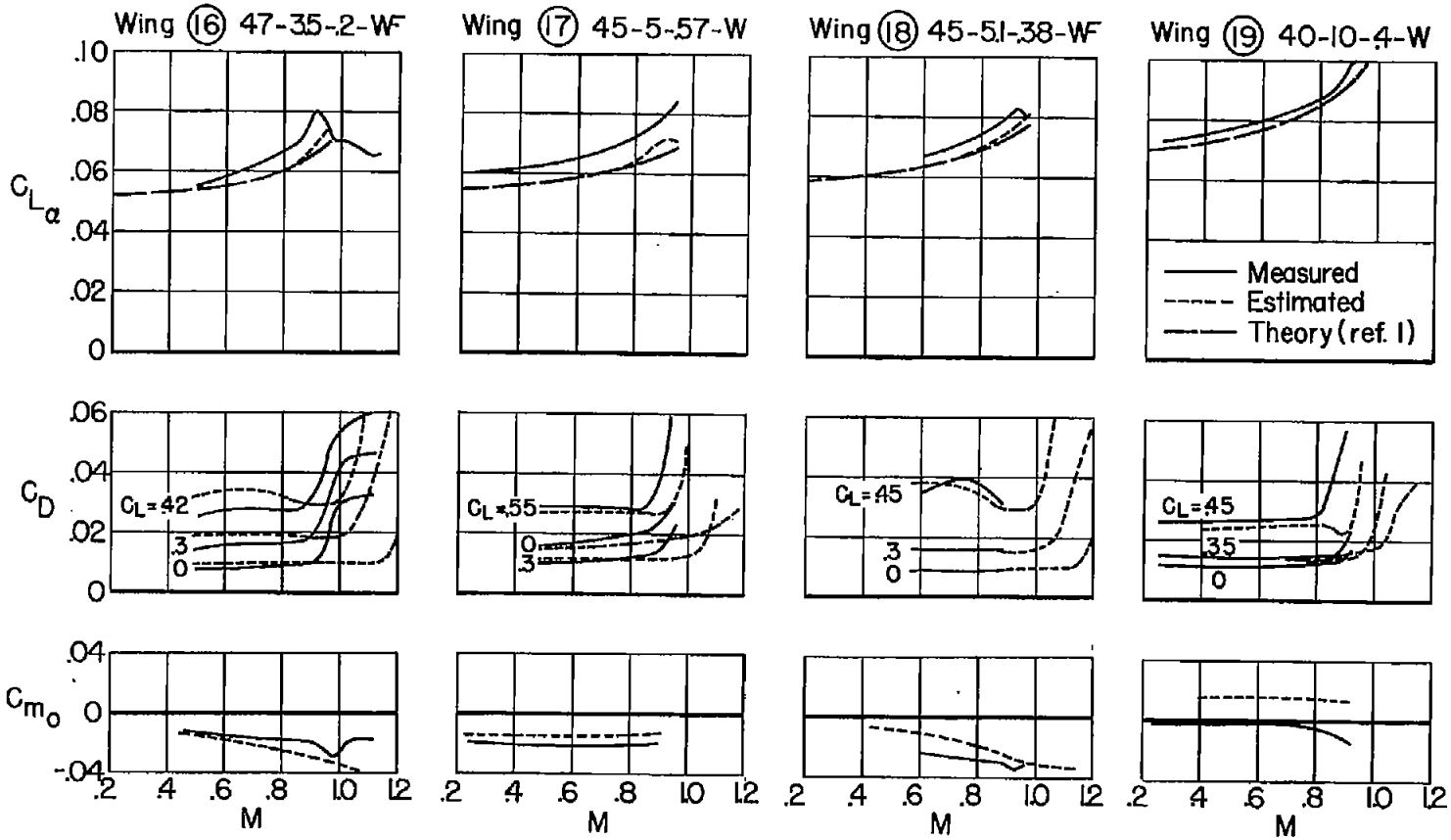

(f) Wings 16 to 19

Figure 1.- Continued.

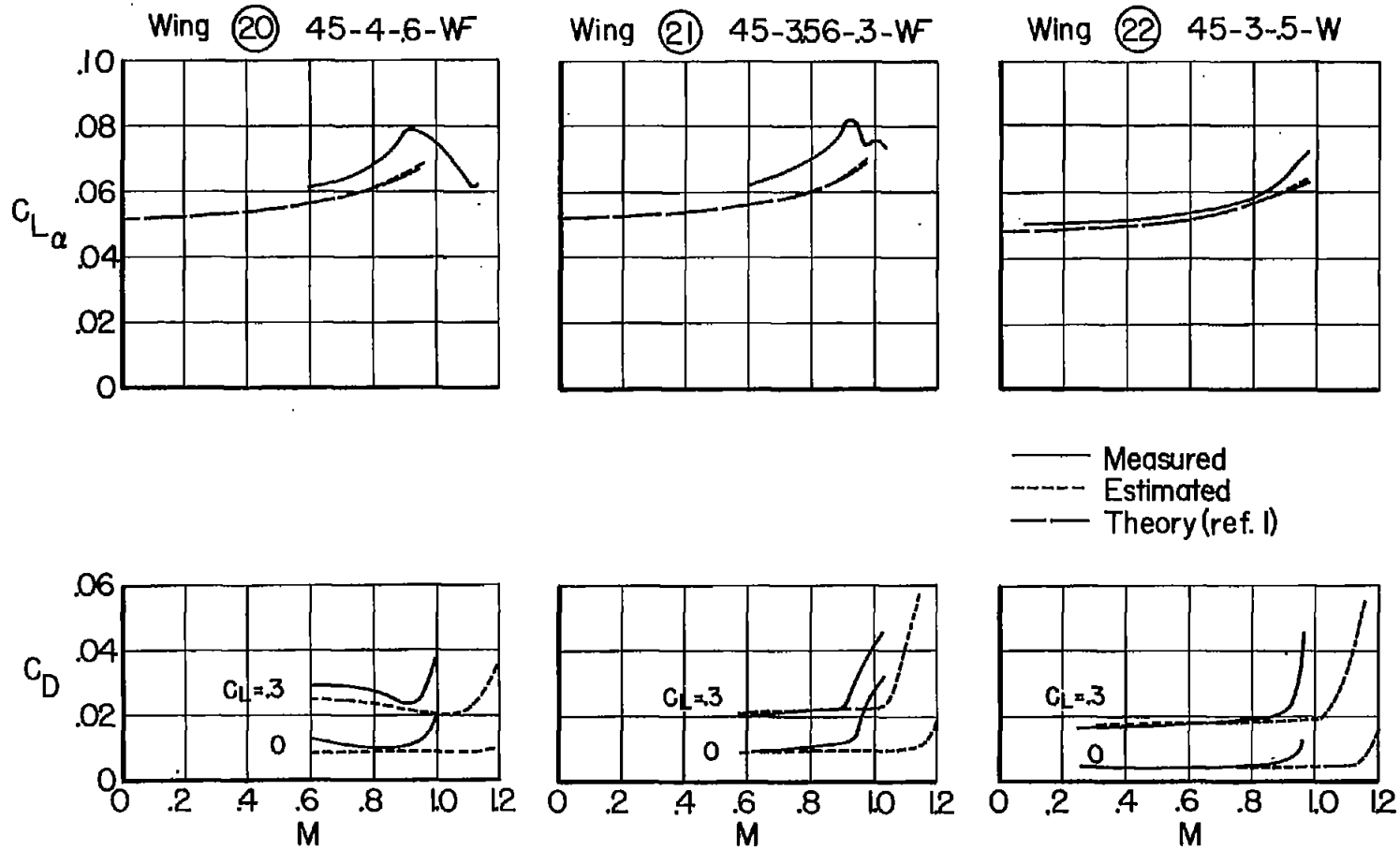

(g) Wings 20 to 22

Figure 1.- Continued.

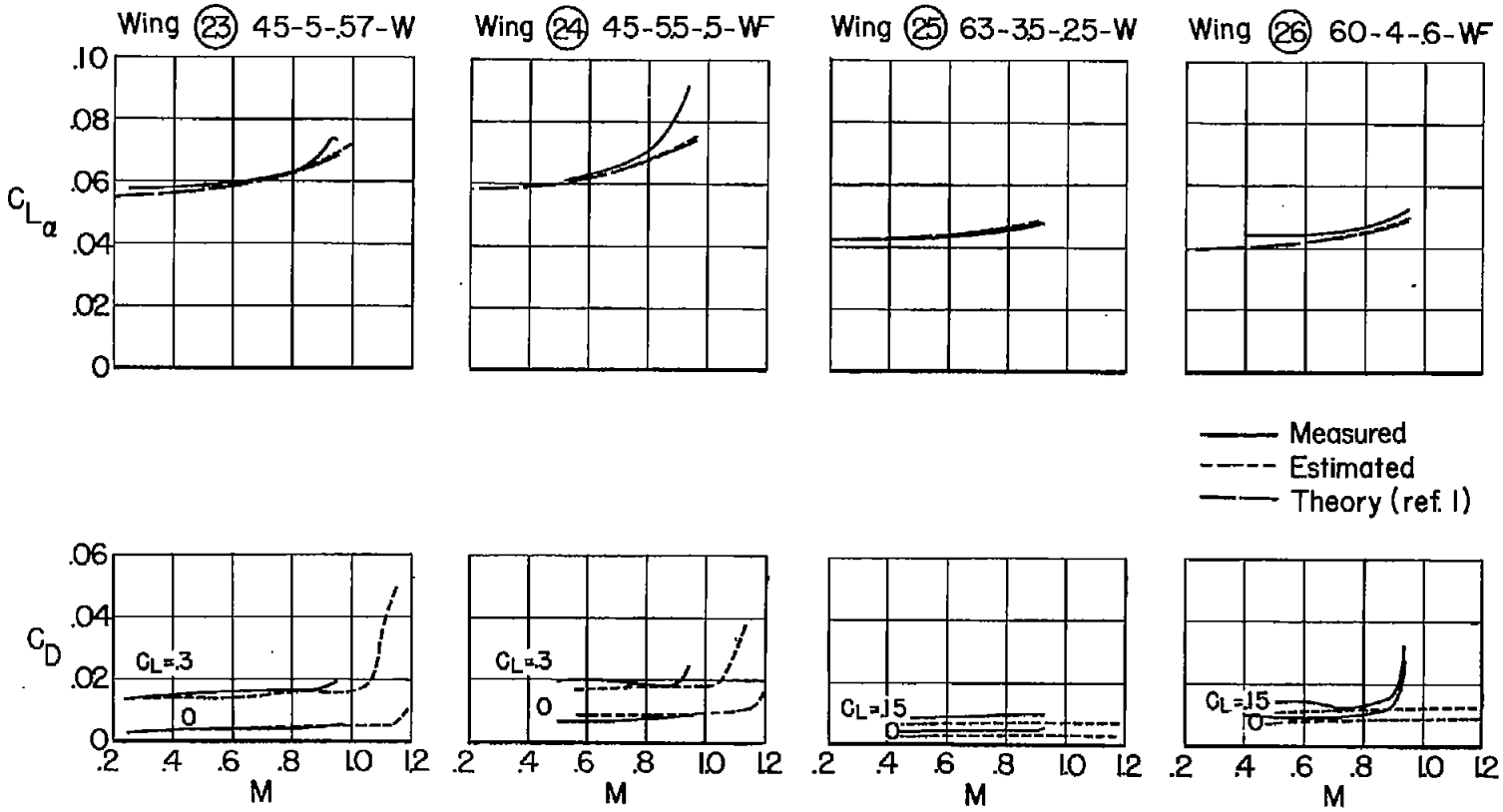

(h) Wings 23 to 26

Figure 1.- Concluded.

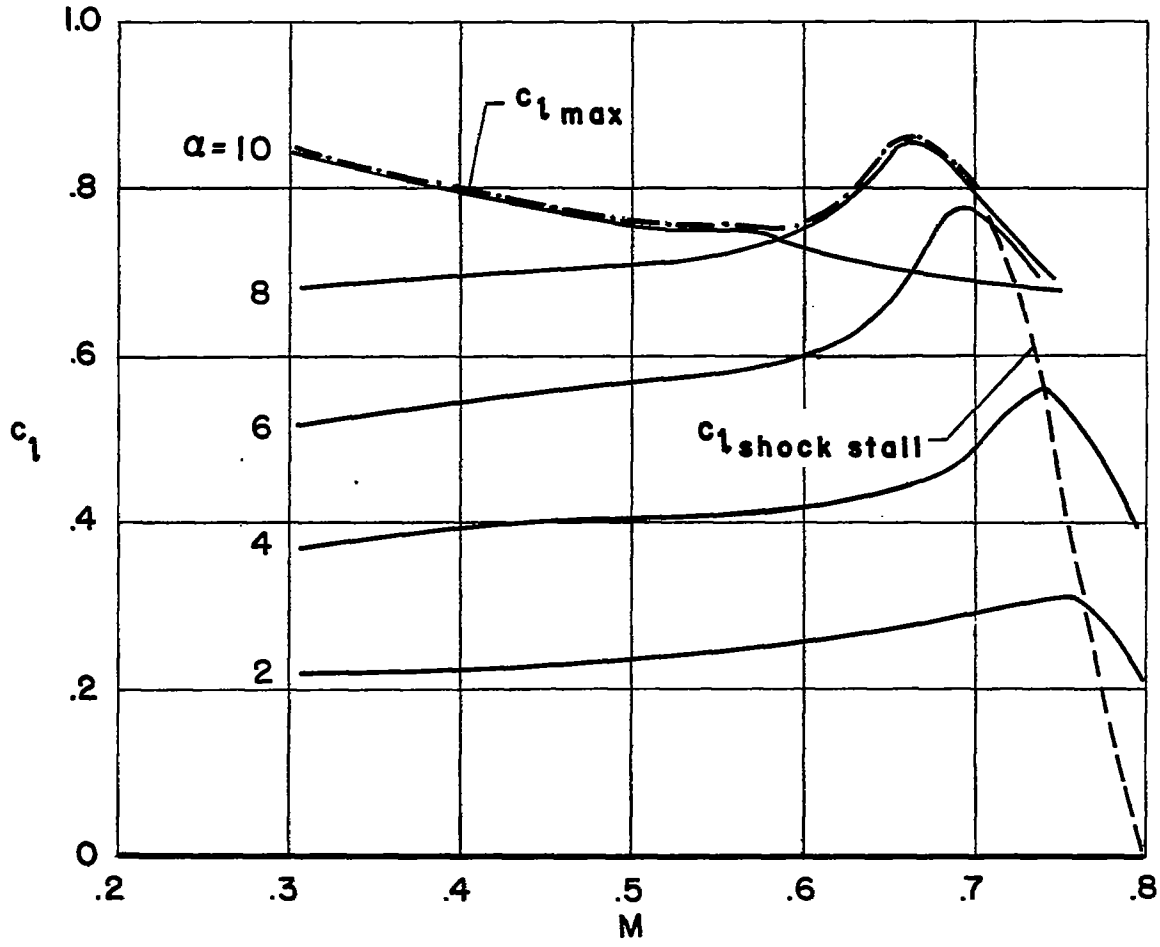

Figure 2.- Variation of section lift coefficient with Mach number at constant angle of attack for the airfoil section of wing 5; R ≈ 1.6 million.

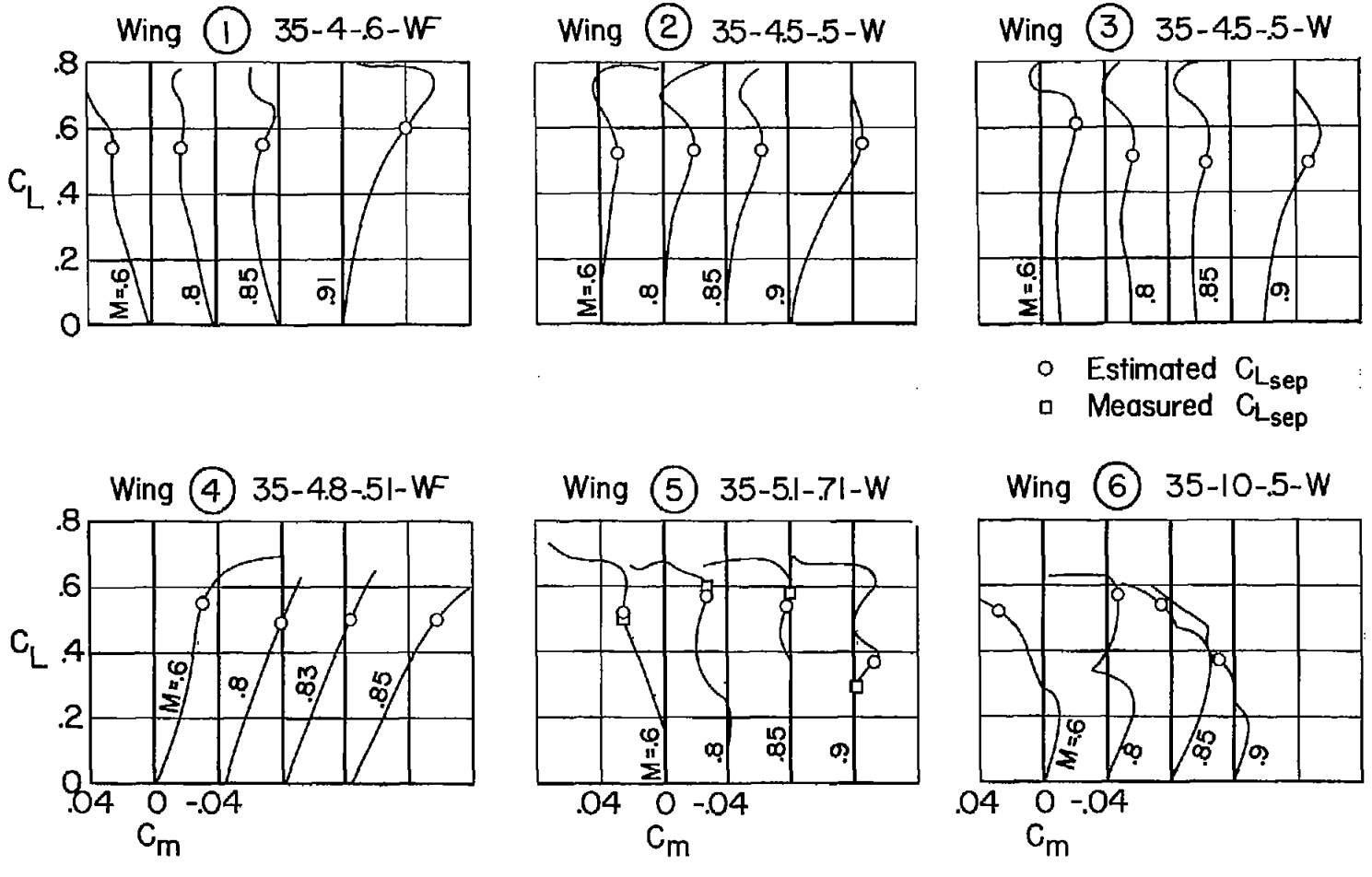

(a) Wings 1 to 6

Figure 3.- Correlation of the estimated values of lift coefficient for trailing-edge flow separation with the measured pitching-moment characteristics.

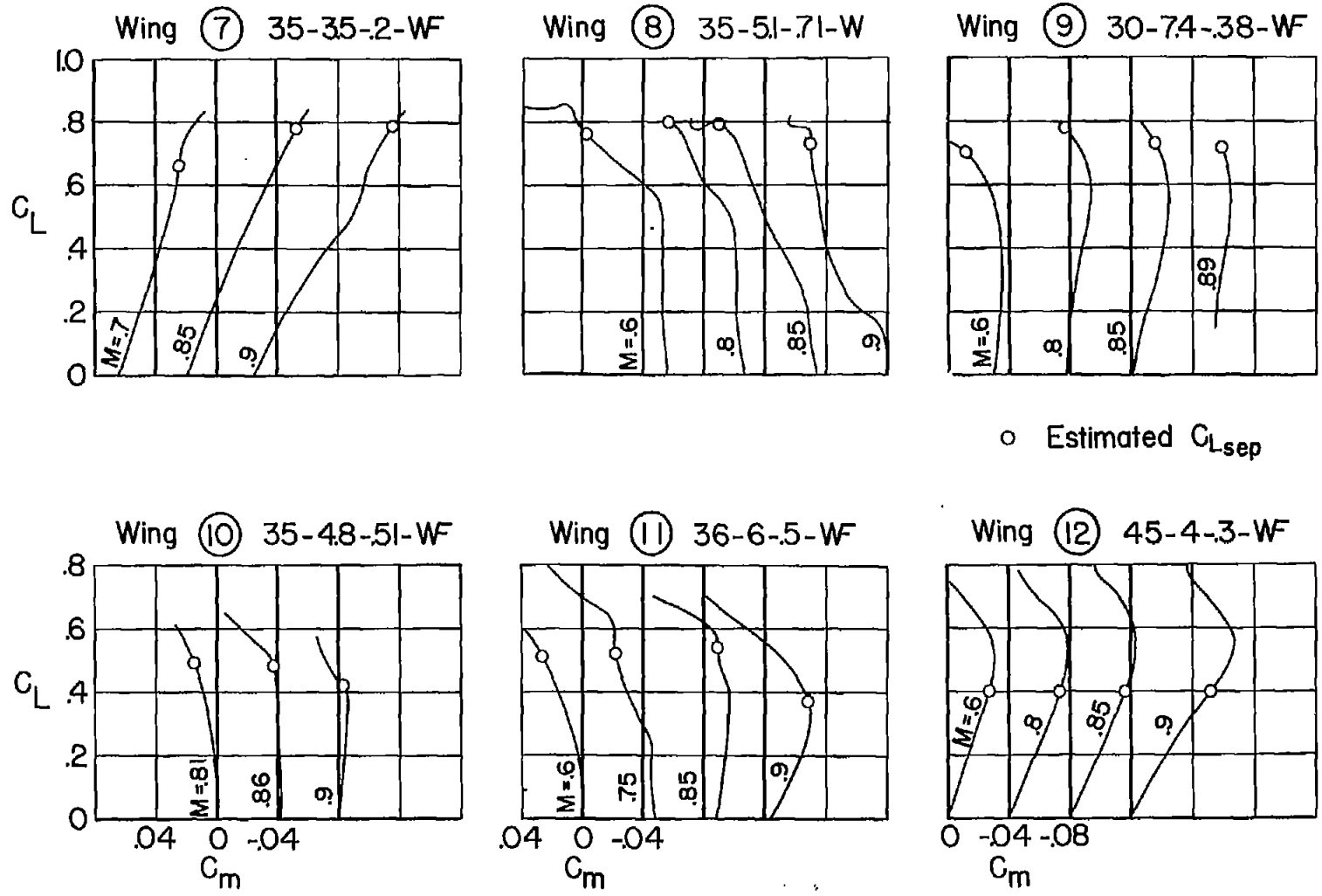

(b) Wings 7 to 12

Figure 3.- Continued.

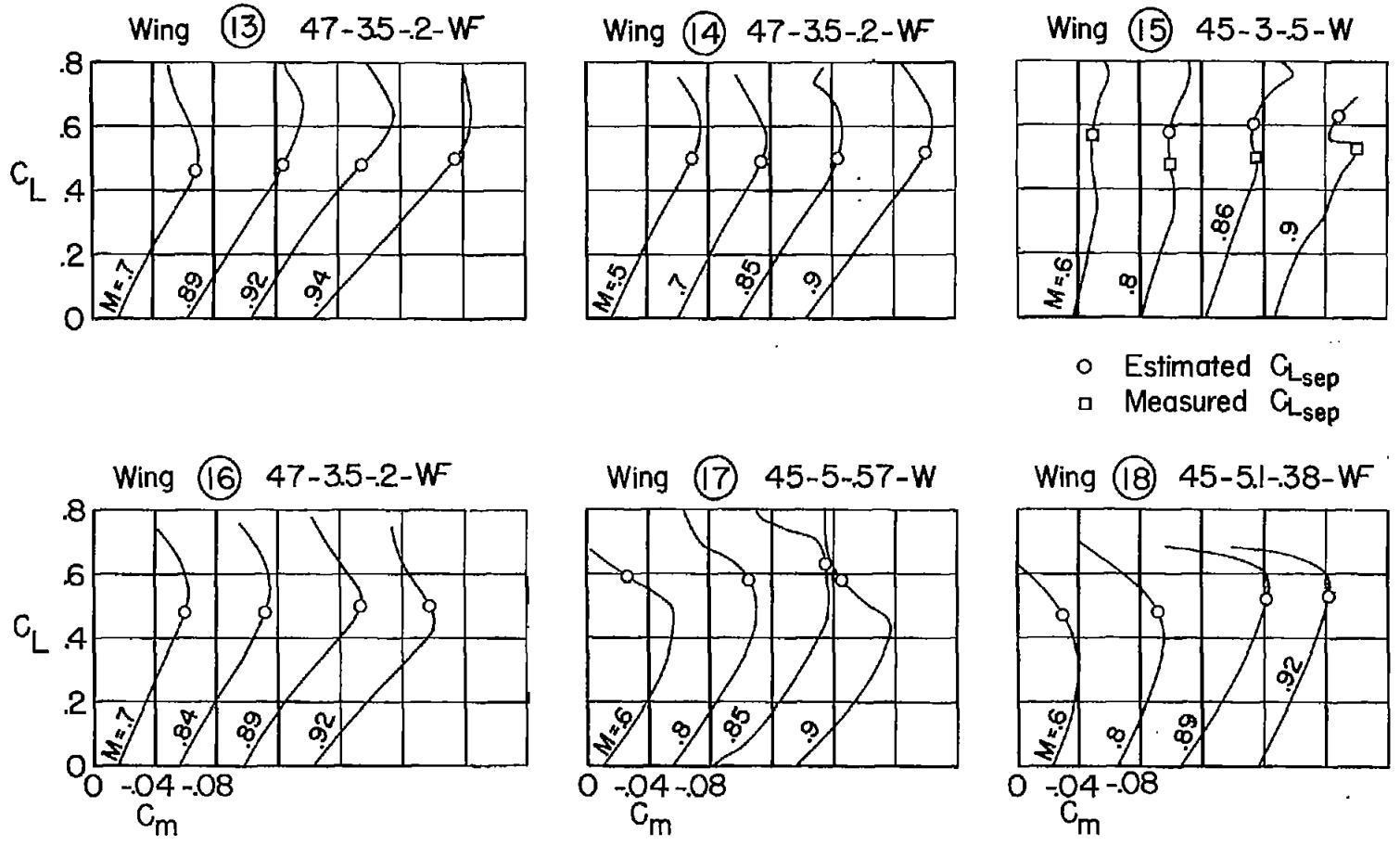

(c) Wings 13 to 18

Figure 3.- Continued.

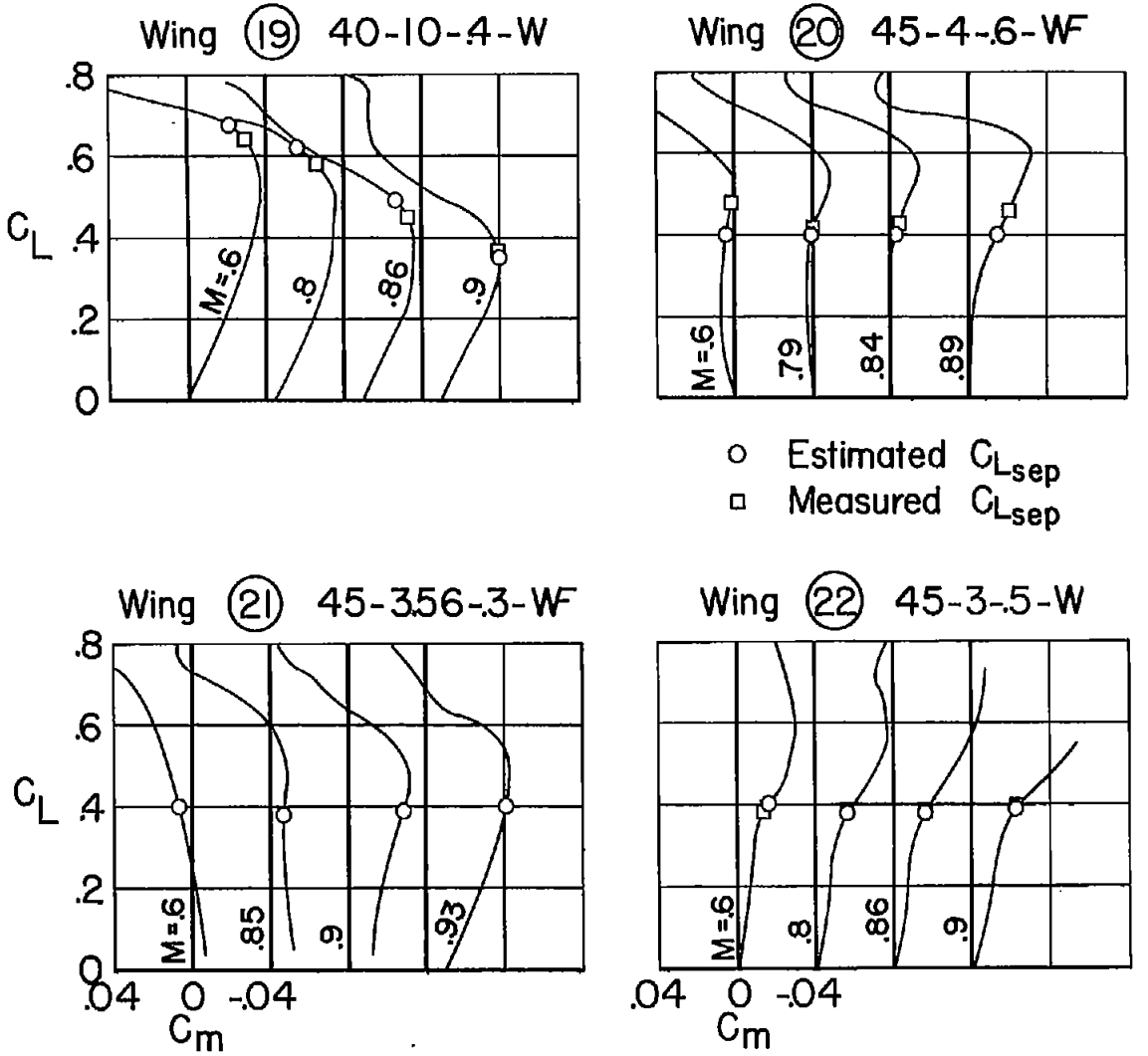

(d) Wings 19 to 22

Figure 3.- Continued.

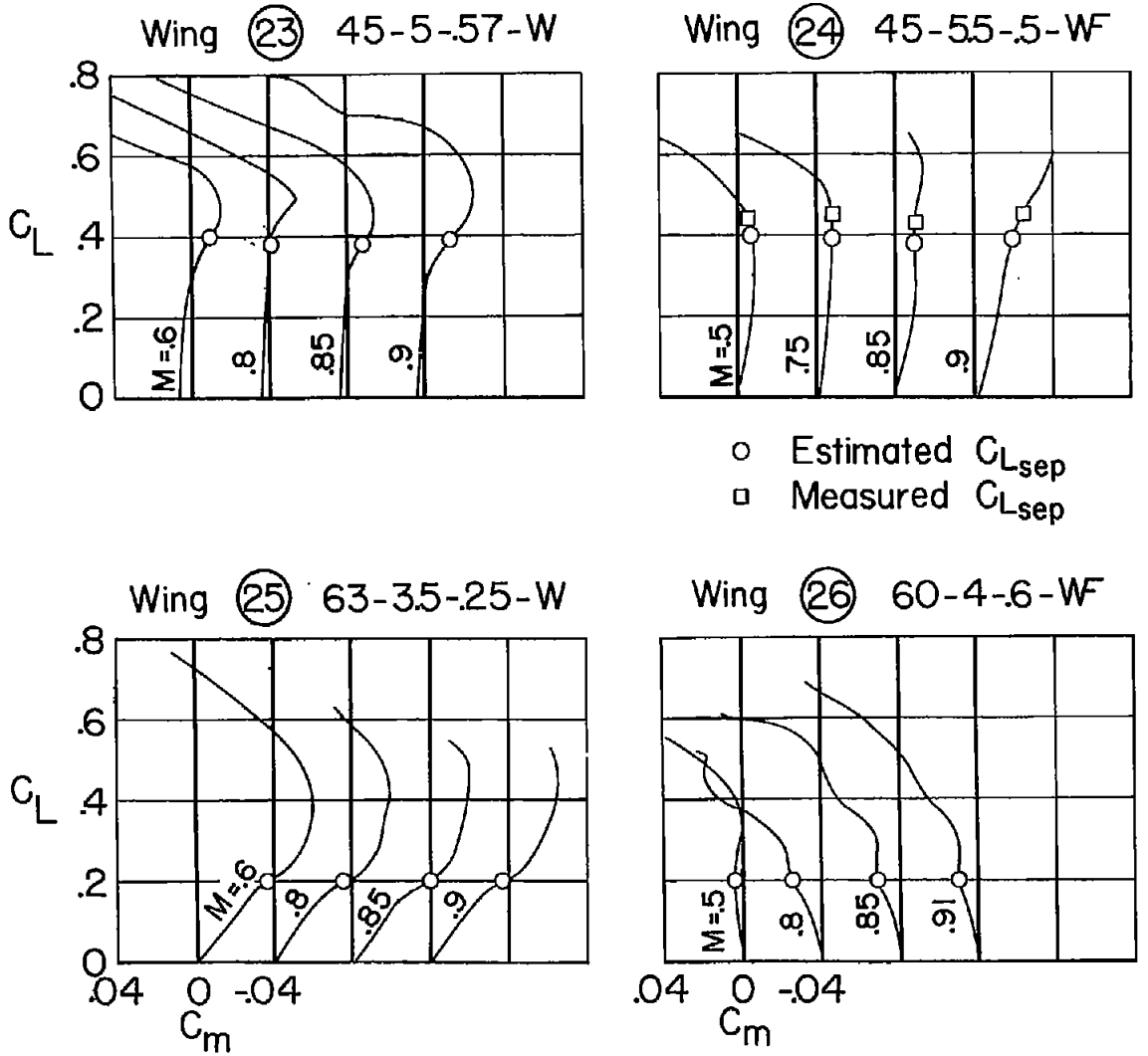

(e) Wings 23 to 26

Figure 3.- Concluded.

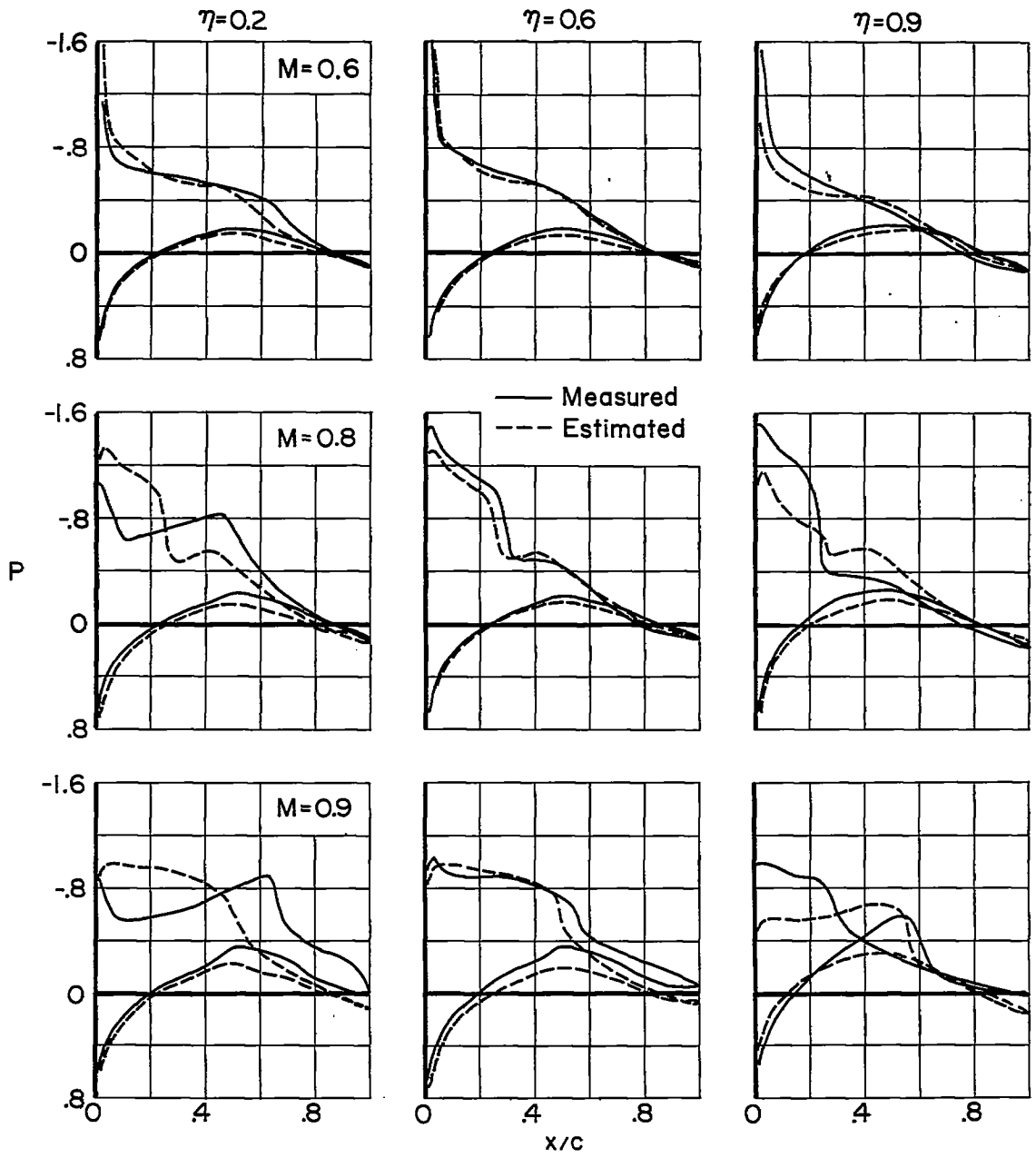

Figure 4.- Comparison of the estimated and measured pressure distributions for sections of wing 5; $\alpha = 6^{\circ}$.

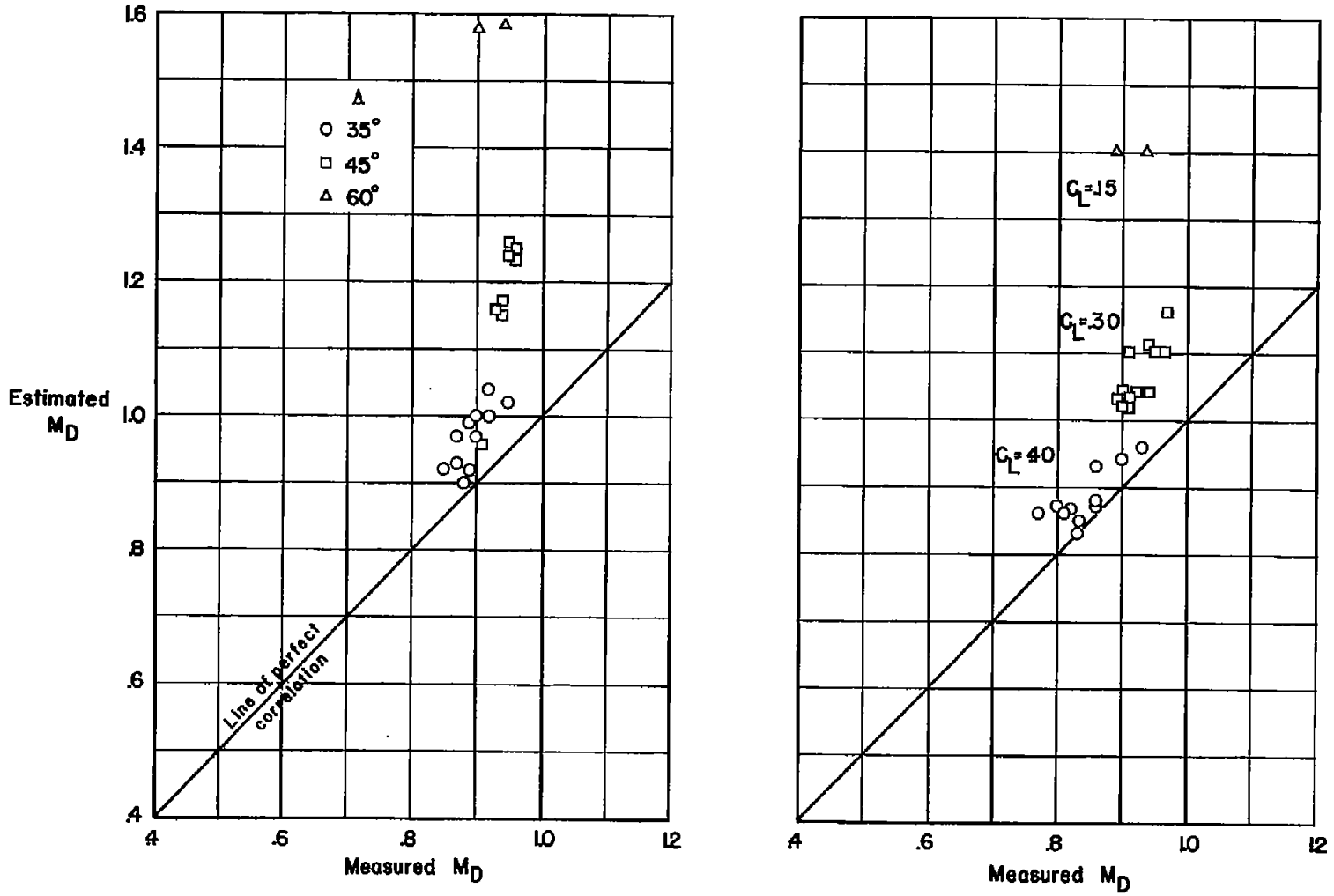

(a) $C_L = 0$

(b) C_L variable

Figure 5.- Comparison of the measured and estimated values of drag-divergence Mach number determined by the adjusted wing theory procedure.

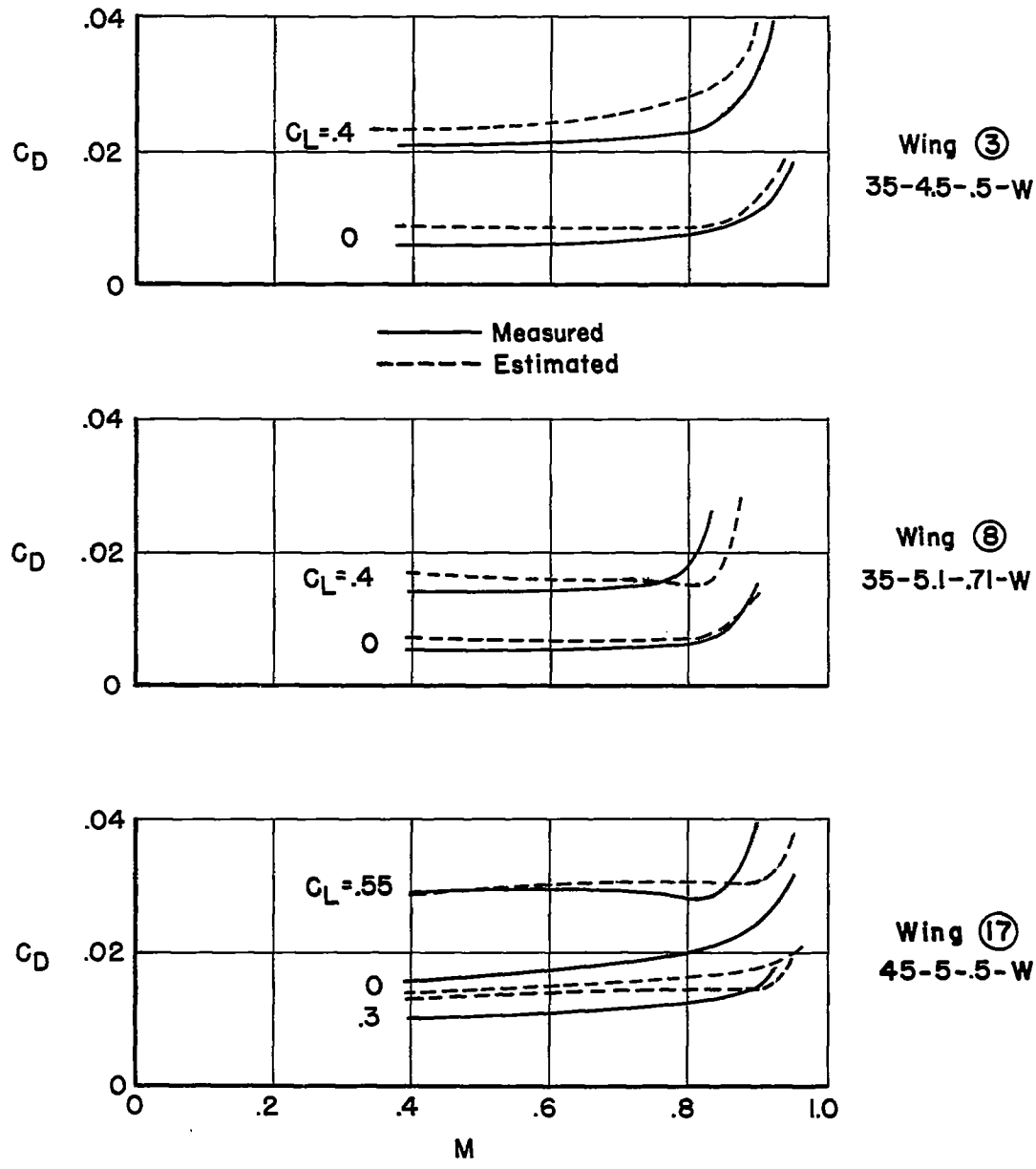

(a) Wings 3, 8, and 17

Figure 6.- Comparison of the measured and estimated variation of drag coefficient with Mach number determined by the adjusted wing data procedure.

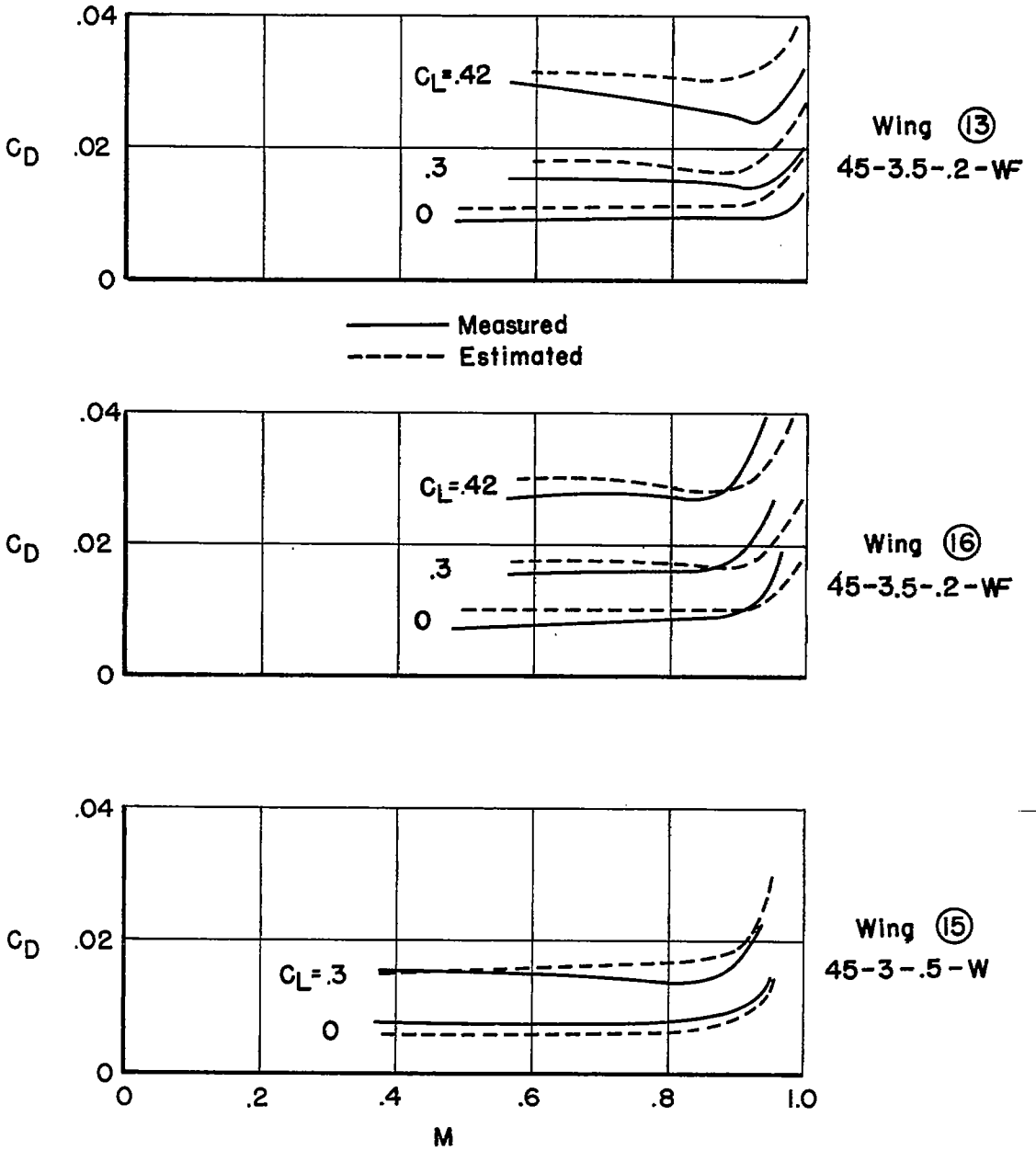

(b) Wings 13, 16, and 15

Figure 6.- Concluded.

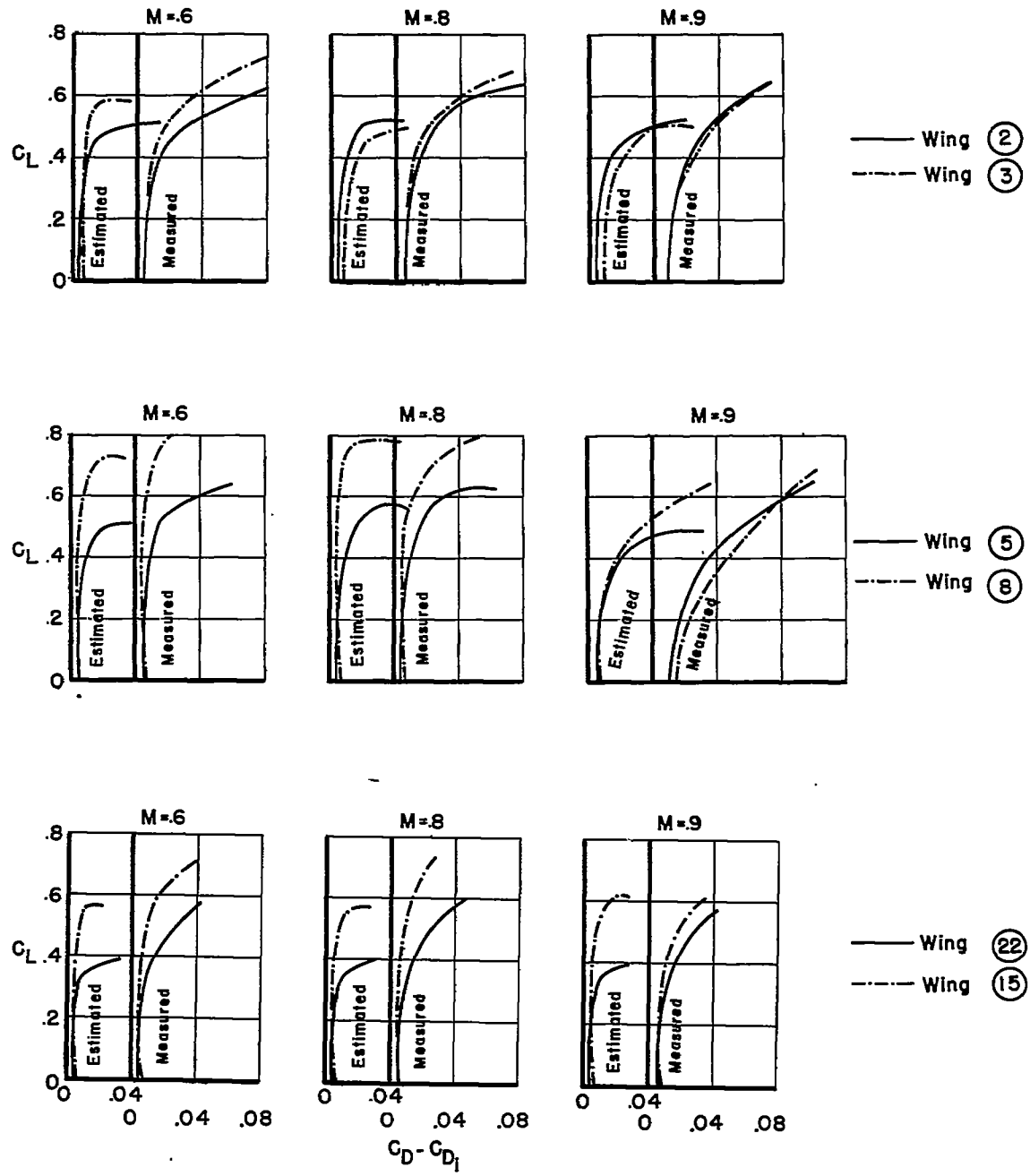

(a) Wings 2, 3, 5, 8, 22 and 15

Figure 7.- Comparison of the measured and estimated variations of profile-drag coefficient with lift coefficient.

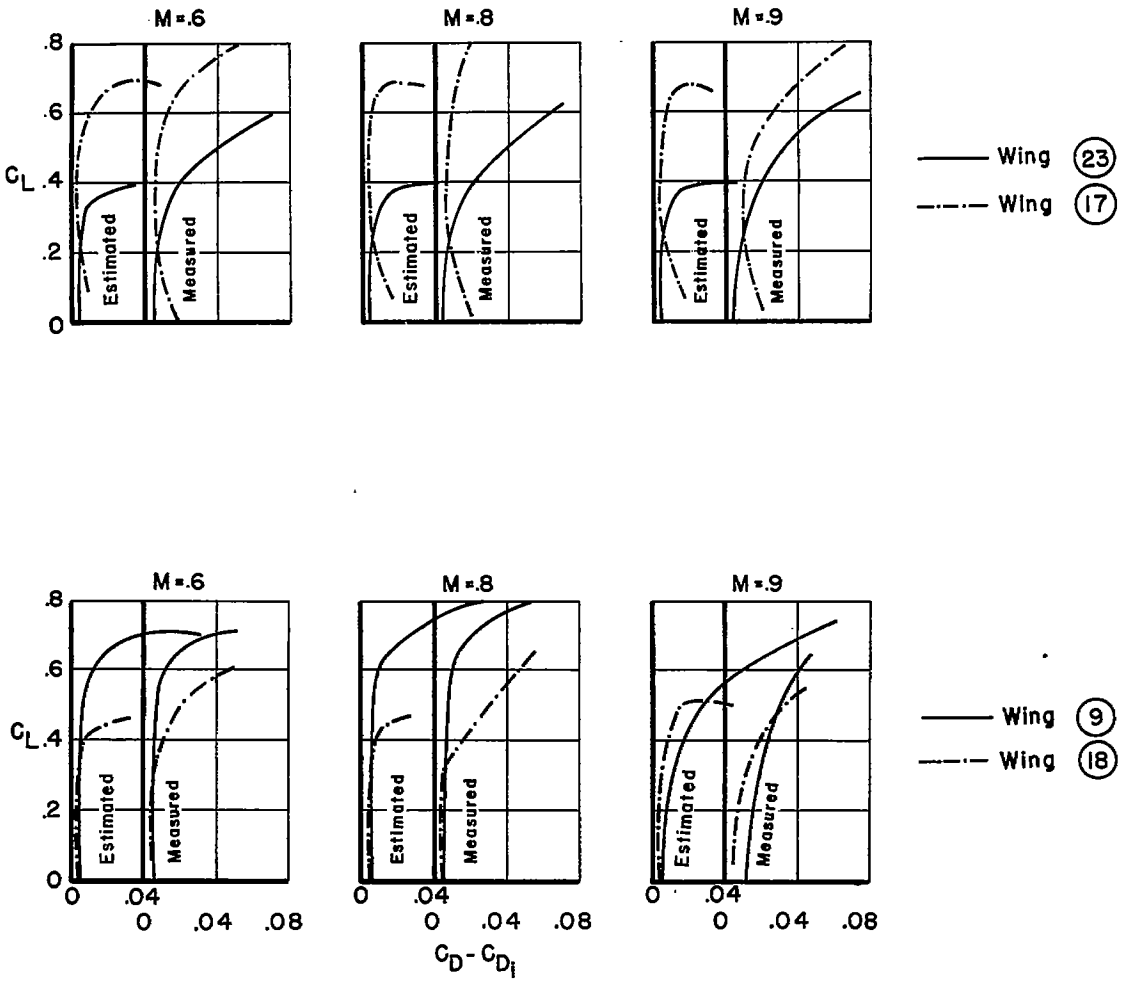

(b) Wings 23, 17, 9 and 18

Figure 7.- Concluded.

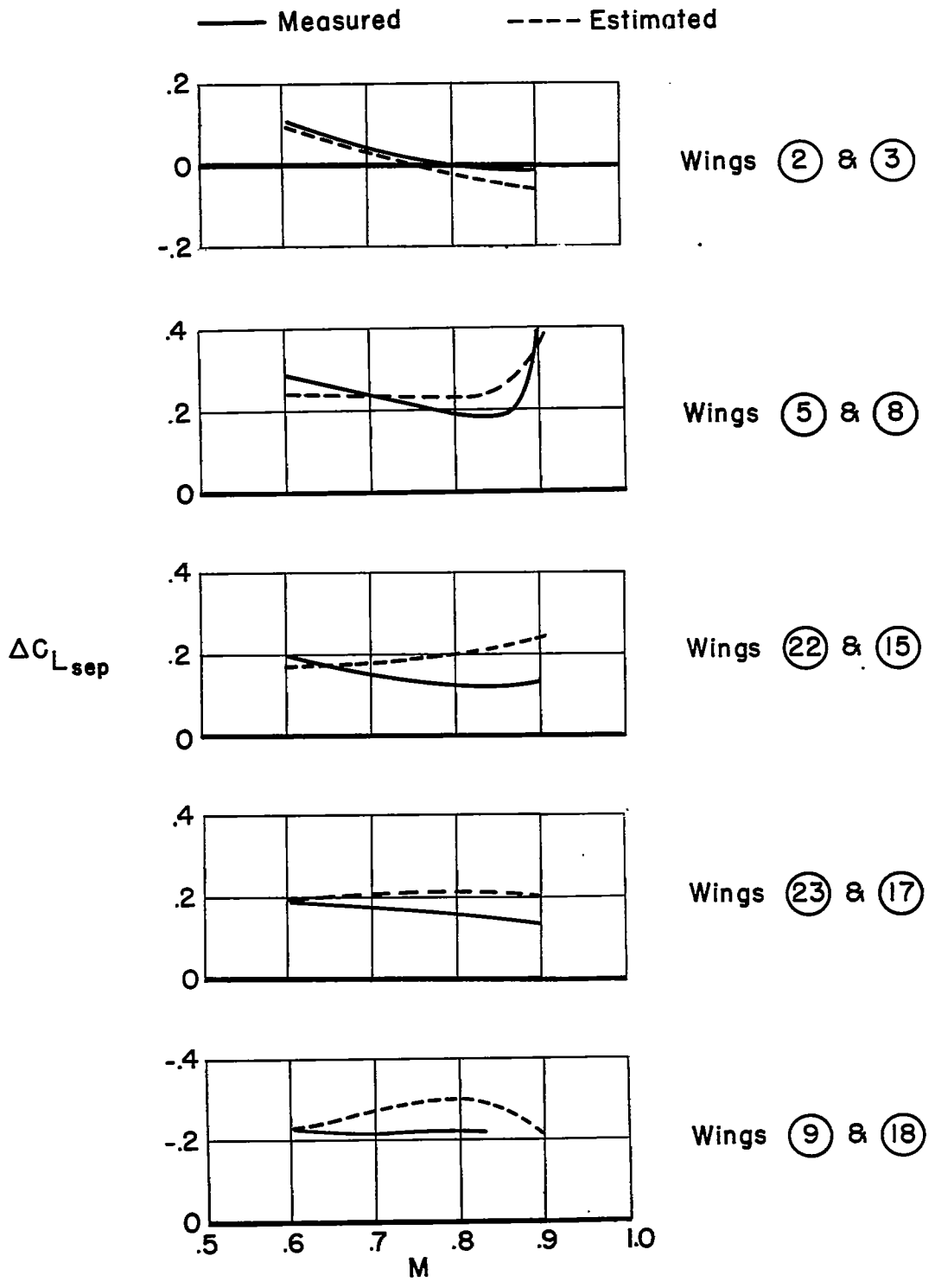

Figure 8.- Comparison of the measured and estimated incremental changes in lift coefficient for flow separation.

NACA-Langley - 6-24-55 - 350